

RESEARCH ARTICLE

The *MITF* paralog *tfec* is required in neural crest development for fate specification of the iridophore lineage from a multipotent pigment cell progenitor

Kleio Petratou^{1‡}, Samantha A. Spencer², Robert N. Kelsh^{1*}, James A. Lister²

1 Department of Biology and Biochemistry and Centre for Regenerative Medicine, University of Bath, Bath, United Kingdom, **2** Department of Human and Molecular Genetics and Massey Cancer Center, Virginia Commonwealth University School of Medicine, Richmond, Virginia, United States of America

‡ Current address: Institute for Cardiovascular Organogenesis and Regeneration, Faculty of Medicine, Westfälische Wilhelms-Universität Münster, Münster, Germany

* r.n.kelsh@bath.ac.uk



OPEN ACCESS

Citation: Petratou K, Spencer SA, Kelsh RN, Lister JA (2021) The *MITF* paralog *tfec* is required in neural crest development for fate specification of the iridophore lineage from a multipotent pigment cell progenitor. PLoS ONE 16(1): e0244794. <https://doi.org/10.1371/journal.pone.0244794>

Editor: Michael Klymkowsky, University of Colorado Boulder, UNITED STATES

Received: October 20, 2020

Accepted: November 29, 2020

Published: January 13, 2021

Copyright: © 2021 Petratou et al. This is an open access article distributed under the terms of the [Creative Commons Attribution License](https://creativecommons.org/licenses/by/4.0/), which permits unrestricted use, distribution, and reproduction in any medium, provided the original author and source are credited.

Data Availability Statement: All original count data files are available from the following site: (<https://doi.org/10.15125/BATH-00743>).

Funding: This work was supported by the University of Bath (KP, RNK) within the Biotechnology and Biological Sciences Research Council (BBSRC; <https://bbsrc.ukri.org/>)-funded South West Biosciences Doctoral Training Partnership, by BBSRC grant BB/L00769X/1 (RNK), and by a National Institutes of Health Clinical and Translational Science Award

Abstract

Understanding how fate specification of distinct cell-types from multipotent progenitors occurs is a fundamental question in embryology. Neural crest stem cells (NCSCs) generate extraordinarily diverse derivatives, including multiple neural, skeletogenic and pigment cell fates. Key transcription factors and extracellular signals specifying NCSC lineages remain to be identified, and we have only a little idea of how and when they function together to control fate. Zebrafish have three neural crest-derived pigment cell types, black melanocytes, light-reflecting iridophores and yellow xanthophores, which offer a powerful model for studying the molecular and cellular mechanisms of fate segregation. *Mitfa* has been identified as the master regulator of melanocyte fate. Here, we show that an *Mitf*-related transcription factor, *Tfec*, functions as master regulator of the iridophore fate. Surprisingly, our phenotypic analysis of *tfec* mutants demonstrates that *Tfec* also functions in the initial specification of all three pigment cell-types, although the melanocyte and xanthophore lineages recover later. We show that *Mitfa* represses *tfec* expression, revealing a likely mechanism contributing to the decision between melanocyte and iridophore fate. Our data are consistent with the long-standing proposal of a tripotent progenitor restricted to pigment cell fates. Moreover, we investigate activation, maintenance and function of *tfec* in multipotent NCSCs, demonstrating for the first time its role in the gene regulatory network forming and maintaining early neural crest cells. In summary, we build on our previous work to characterise the gene regulatory network governing iridophore development, establishing *Tfec* as the master regulator driving iridophore specification from multipotent progenitors, while shedding light on possible cellular mechanisms of progressive fate restriction.

(UL1TR000058 from the National Center for Advancing Translational Sciences) to Virginia Commonwealth University and the AD Williams' Fund of Virginia Commonwealth University (SS, JAL). The funders had no role in study design, data collection and analysis, decision to publish, or preparation of the manuscript.

Competing interests: The authors have declared that no competing interests exist.

Introduction

Pigmentation is a conspicuous feature of animal diversity and has broad importance for behaviour and evolution (reviewed in [1]). Much is known about the development and cell biology of melanocytes but far less is understood about the genetic mechanisms underlying the diversity of pigment cell types in non-mammalian vertebrates. Zebrafish embryos display three neural crest (NC)-derived pigment cells: melanophores, melanin-producing cells homologous to the melanocytes of mammals, and often referred to simply as melanocytes; xanthophores, yellow-orange cells bearing pteridine and carotenoid pigments; and iridophores, shiny cells containing platelets composed of guanine (reviewed in [2, 3]). Defining the fate specification mechanisms of these other cell-types is important for understanding both their genetic control and the evolutionary origins of vertebrate pigmentation, but also the much-debated process of neural crest cell (NCC) fate restriction.

The progressive fate restriction model proposes that neural crest cells (NCCs) become partially fate restricted as development progresses, giving rise to intermediate partially-restricted progenitors, each of which can generate a number, but not all of the NC derivatives [4–8]. Such a model has been strongly supported for the neural derivatives by a single cell transcriptional profiling study in mice, although, surprisingly it was unable to resolve pigment cell development [9]. Although the progressive fate restriction model has been supported by a number of studies using zebrafish, the number and identity or, indeed, even the existence of intermediate progenitors remains unclear [10–12]. Work to define the gene regulatory networks underlying fate choice provides an important context for these cellular mechanisms [11, 13, 14].

Characterisation of the phenotypes of mutants affecting multiple NC derivatives has been widely used to infer the identities and potencies of these progenitors. In the pigment cell field, a progressive fate restriction model has been developed based on loss- and gain-of-function studies for single genes, with both a multipotent chromatoblast and a bipotent melano-iridoblast proposed as partially-restricted intermediates [11, 14–17]. Studies of fate-specification mutants further permits elucidation of the gene regulatory networks (GRNs) governing diversification of these precursors [13, 14].

To date, examination of zebrafish mutants provides evidence of complex genetic control of pigment cell development from multipotent NCCs [18]. Of the genes affected in these mutants, many have been shown to encode transcription factors that regulate fate specification of pigment cells from NCCs. Such factors may be required by either all three pigment cell lineages (e.g. *colourless/sox10*; [19, 20]) or only a single pigment cell lineage (e.g. *nacre/microphthalmia-associated transcription factor a/mitfa*, [21]). Consequently, genetic loss of several transcription factors affects one or more pigment cell types, perhaps indicating the existence of shared progenitors. For example, loss of *sox10* function results in lack of all three zebrafish lineages, but also hinders the development of peripheral nervous system components [22, 23]. Although a tripotent progenitor restricted to generating all chromatophore lineages has long been hypothesised [15], mutants with the expected phenotype (I.e. *restricted* to the three pigment cell lineages alone) have not been identified.

As a first step towards understanding the complex GRN governing NCC fate restriction towards pigment cell lineages, it is important to define the key components involved in fate specification of individual lineages. Of the three zebrafish pigment cells, melanocytes are the currently best studied. In this lineage, Sox10, in conjunction with Wnt signalling, is required to activate and maintain *mitfa* transcription [13, 20, 24–26]. Like its mammalian counterpart, MITF, *Mitfa* has been proven necessary and sufficient to upregulate numerous melanocyte differentiation genes, including those controlling melanin synthesis (e.g. *dct*, *silva* and *tyrosinase*).

Mitfa is thus dubbed the ‘master regulator’ of melanocyte fate choice [13, 21, 25]. However, in this role, Mitfa is supported by Tfap2, especially Tfap2a which acts as a key co-factor [27]. In contrast, Foxd3 mutants show a complex phenotype that includes delayed melanocyte and xanthophore specification and differentiation, ultimately resulting in wild-type cell numbers, and reduced iridophore numbers [16, 28–30]. These phenotypes seem to reflect roles for FoxD3 in both lineage priming [31] and, in certain contexts, repressing melanogenesis promoting the specification of other fates [16, 17].

Recent studies of key zebrafish iridophore mutants have begun to define the basic genetics of this cell type. In terms of their differentiation, heightened purine synthesis is central to the development of the guanine crystals that form the reflecting platelets. Thus, *purine nucleoside phosphorylase 4a* (*pnp4a*), which encodes an enzyme important in the biosynthesis of guanine, is a robust marker of mature iridophores [14, 17]. Additionally, mutations of several enzymes specific to differentiated iridophores have been shown to disrupt purine biosynthesis [32], while disruption of other proteins was found to impair iridophore survival [33–35]. Furthermore, a signalling pathway crucial to fate specification, proliferation and differentiation of iridophores has been highlighted by mutations in the gene encoding the Leukocyte Tyrosine Kinase (Ltk; [11, 36]) receptor tyrosine kinase, with corroboration from targeted loss of function of its ligand [37, 38]. In *shady/ltk* mutants fate specification and proliferation of iridophores, but not other pigment cells, are impeded [11, 36]. Nevertheless, Ltk signalling alone is not sufficient for iridophore specification, since iridophores are eliminated in *sox10* mutants, even though *ltk* expression is strongly detectable by whole-mount *in situ* hybridisation [11, 14]. The function of Ltk signalling in specification of the iridophore lineage is, thus, likely analogous to that of Wnt signalling in generating melanocytes. This then leaves open the question of whether there is a ‘master’ transcriptional regulator of the iridophore lineage, analogous to the role of Mitfa in melanocytes.

The zebrafish “MiT” (Mitt/Tfe) family consists of six genes [39]; of these, *mitfa* and *tfec* are the only ones expressed in the NC. The distinctive expression pattern of *tfec* in cells along the dorsal and ventral midline in the trunk and tail and two patches over the yolk, is strongly reminiscent of differentiating iridophores [39]. Furthermore, Higdon et al. performed transcriptomic analysis to compare FACS-purified iridophores, melanocytes, and retinal pigment epithelium (RPE), and found *tfec* to be one of several transcription factor genes with enriched expression specifically in the iridophore lineage [40]. Together, these data lead to the hypothesis that Tfec might be the iridophore master regulator, equivalent to Mitfa in developing melanocytes.

In a recent detailed study, we demonstrated that, indeed, *tfec* serves as a robust marker of the iridophore lineage, allowing us to define the major stages of iridophore development [14] (Fig 1). Based on whole-mount *in situ* hybridisation studies of *tfec* expression patterns throughout a developmental time-course, and co-expression analysis with both *ltk* and *mitfa*, we concluded that *tfec* is first expressed extensively throughout the premigratory NC progenitors of the trunk and tail at 18 hpf, and then exclusively in the developing iridophore lineage. Focussing on cells in the posterior trunk, we distinguished a subset of *tfec*-positive cells within the premigratory domain that have downregulated the early NCC marker, *foxd3*, but do not express definitive pigment cell markers; we refer to these as early chromatoblasts (Fig 1; *Cbl early*). At approximately 22 hpf, *ltk* and *mitfa* are upregulated in the *tfec*+; *foxd3*- premigratory cells of the trunk [11, 14, 21], indicating that they correspond to partially restricted progenitors, capable of generating pigment cells (Fig 1; *Cbl late*). By 24 hpf, *tfec* labels migrating progenitors which co-express *mitfa* and *ltk* markers, and which we consider fate-specified iridoblasts, but which likely retain at least melanocyte potential too (Fig 1; *Ib(sp)*; [14]). From 30 hpf, *tfec*+ cells co-express *ltk*, but not *mitfa*, and we now consider these to be either

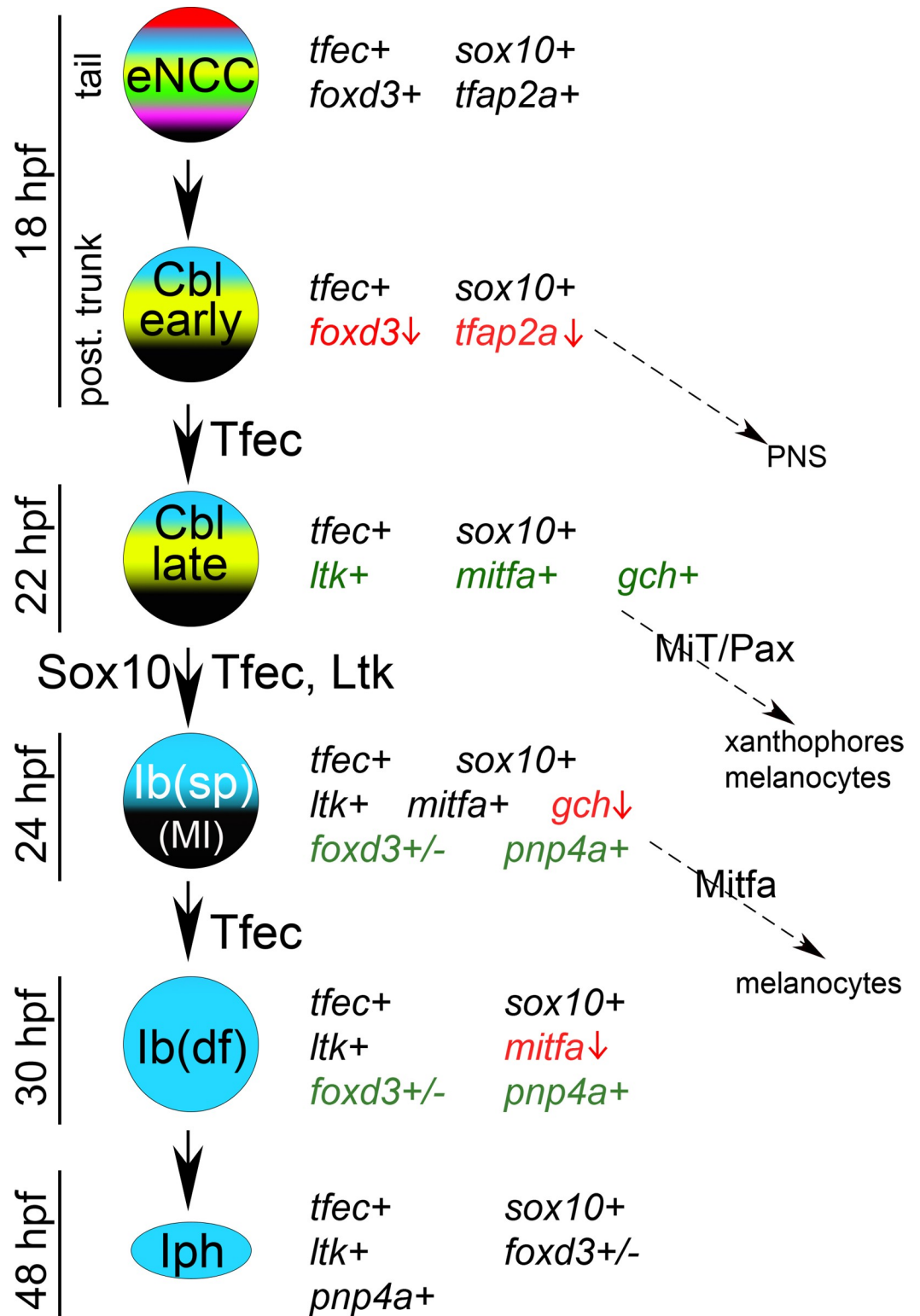


Fig 1. A progressive fate restriction model for iridophore development from multipotent NCCs. Schematic representation of the previously described model of iridophore generation from the NC, along with the expression characteristics and potential fate choices of individual arising cell types [14]. Genes actively expressed in each cell are indicated with a “+” sign. *tfec* is initially co-expressed with eNCC specification factors, which gradually become downregulated (red font, vertical red arrow), while lineage-specific factors become upregulated (green font). Proteins

indicated on the vertical black arrows are considered important for the respective fate specification step. MiT, microphthalmia family transcription factors; PNS, peripheral nervous system.

<https://doi.org/10.1371/journal.pone.0244794.g001>

definitive iridoblasts (Fig 1; *Ib(df)*), along the dorsal trunk and on the lateral migration pathway at 30 hpf), or mature iridophores (in iridophore locations from 42 hpf onwards) according to their position and state of visible differentiation. Thus, the established iridophore-associated expression pattern of *tfec* during zebrafish development reinforces the hypothesis that Tfec might act as the missing iridophore master regulator, but does not eliminate the possibility of additional earlier functions, either in multipotent early NCCs (eNCCs; Fig 1), or in partially restricted precursors with wider potencies.

In our previous study we used a preliminary assessment of *tfec* mutants to inform our derivation of a core iridophore GRN. Here, we describe in detail the generation and comprehensive characterization of the effects on NC development of mutations in *tfec*. Following examination of the development of a wide variety of NC derivatives in *tfec* mutants, using early and late molecular markers, we conclude that, although neuronal and skeletal derivatives develop normally, specification of *all* pigment cell fates is delayed in homozygous mutants, suggesting a common early requirement for *tfec* in the GRN governing specification of all three chromatophore lineages, and providing support for a common chromatoblast precursor. Finally, our previous work identified the GRN governing maintenance of *tfec* in the iridophore lineage [14]. In the present study, we extend this work to define *tfec* as a necessary regulator of iridophore specification, yet not alone sufficient to drive NCCs to adopt an iridophore fate. Importantly, we identify its upstream regulators in the multipotent premigratory NC, thus for the first time placing the transcription factor in context in the NCC specification GRN [41]. Together, these data shed light on the possible mechanism of progressive fate segregation of NCCs, and begin to elucidate the complex role for Tfec, being indispensable for iridophore development, but also playing subsidiary roles in specification of the other two chromatophores derived from the zebrafish NC.

Results

tfec is a candidate for the iridophore master regulator

As we showed previously [14], *tfec* is co-expressed with the established iridophore marker, *ltk* [11], during iridoblast fate choice and iridophore differentiation. Although Higdon et al showed that *tfec* expression was prominent in the RNA-seq profiles of iridophores, they also detected low levels of expression in purified melanocytes [40]. Here we used whole-mount *in situ* hybridisation to detect *tfec* in individual embryos, following photographic documentation of their individual iridophore patterns, to show definitively its presence in differentiated iridophores (Fig 2). *tfec* is maintained in differentiated cells (Fig 2A–2D). At these stages, consistent with our previous observations showing no overlap of *tfec* and the melanocyte marker *mitfa* in differentiated melanocytes [14], we do not detect expression in neighbouring differentiated melanocytes occupying the dorsal and ventral stripes (Fig 2A–2D). Likewise, xanthophores, which are widespread under the epidermis of the flanks of the embryos, also do not show detectable *tfec* expression in these expression studies (Fig 2A–2D). To confirm this, we used the xanthophore lineage marker, Pax7, detected via an immunofluorescence assay combined with simultaneous labelling of *tfec* transcript via whole-mount *in situ* hybridisation (Fig 2E–2G). In conclusion, at the detection threshold of our expression studies, *tfec* is a consistent marker of mature iridophores, but not of melanocytes nor xanthophores.

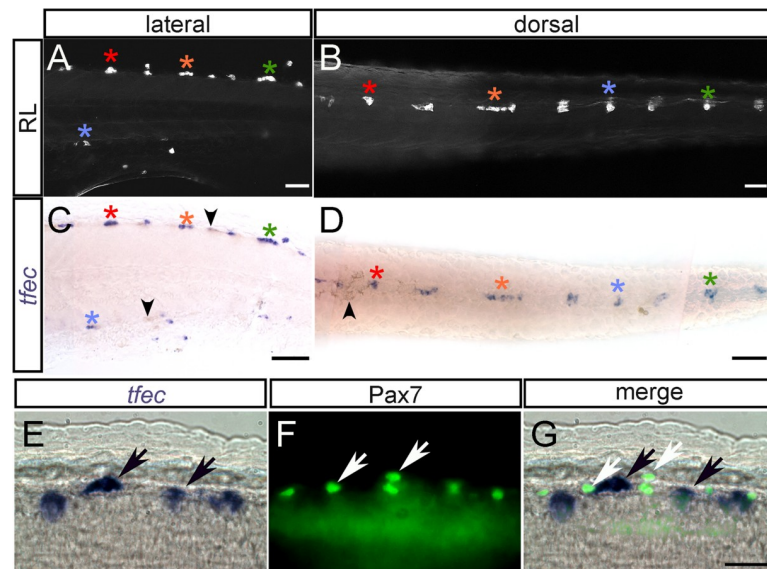


Fig 2. *tfec* is a marker of differentiated iridophores, but not xanthophores. (A–D) Chromogenic whole-mount *in situ* hybridisation reveals *tfec* expression in iridophores (asterisks) of the posterior trunk/anterior tail are imaged live with reflected light in lateral (A) and dorsal (B) views. (C,D) Whole-mount *in situ* hybridisation on the same embryo reveals a pattern of *tfec* expression matching that of the differentiated iridophores (asterisks). The colour of the asterisks indicates corresponding iridophore patches between A and C, and B and D. Note the absence of expression in the location of the associated melanocytes (residual melanin indicated by arrowheads) (E–G). Expression of *tfec* (E, *in situ* hybridisation) and of Pax7 (F, immunofluorescence) in differentiated iridophores and xanthophores, respectively, at 48 hpf; note the absence of co-expression of these markers. A,C,E: lateral views; B,D: dorsal views. Head towards the left. Scale bars: A–D, 50 μ m; E–G, 20 μ m.

<https://doi.org/10.1371/journal.pone.0244794.g002>

Loss of *tfec* function affects the development of all embryonic pigment cells

To assess the role of *tfec* in development, we induced mutations in *tfec* using CRISPR/Cas9 (Fig 3), selecting a target in the seventh exon of the gene, which encodes the second helix of the transcription factor's helix-loop-helix dimerization domain. Our two laboratories independently generated identical 6 base pair deletions (the *tfec*^{ba6} and *tfec*^{vc58} alleles) in two different wild-type strains, WIK and NHGRI-1, in addition to frameshifted alleles (Fig 3A). We reasoned that in this region of the gene it was likely that even indels that retained the correct reading frame (i.e., multiples of three) would likely be deleterious, because they would alter spacing of key residues and surfaces within this helix. Indeed, all of the generated alleles, when made homozygous, resulted in elimination of differentiated iridophores from the dorsal, ventral and yolk sac stripes, as well as from the lateral patches of the embryo (Fig 3B–3E). In addition, iridophores were absent from the dorsal head (Fig 3C and 3E) and the eye (Fig 3B–3E) of homozygous mutants. Moreover, both injected (G0) fish raised to adulthood, as well as a single 'escaper' surviving F1 adult carrying biallelic frameshift mutations, lack iridophores in patches or in whole, indicating an ongoing role in adult iridophores (S1A–S1C Fig). When concerning embryonic stages, all results presented here were produced using either the *tfec*^{ba6} or the *tfec*^{vc60} alleles. The aforementioned alternative frameshift alleles were only used to describe adult phenotypes, because homozygous carriers of both *ba6* and *vc60* never survive to adulthood.

Quantification of iridophore numbers along the dorsal and ventral stripes of live embryos at 3 dpf illustrates the severity of the phenotype, with only very rare escaper iridophores present in homozygous *tfec*^{ba6} mutant embryos (Fig 3F and S1 Table). The numbers of differentiated cells in heterozygous mutants are not significantly different from those in wild-type (WT)

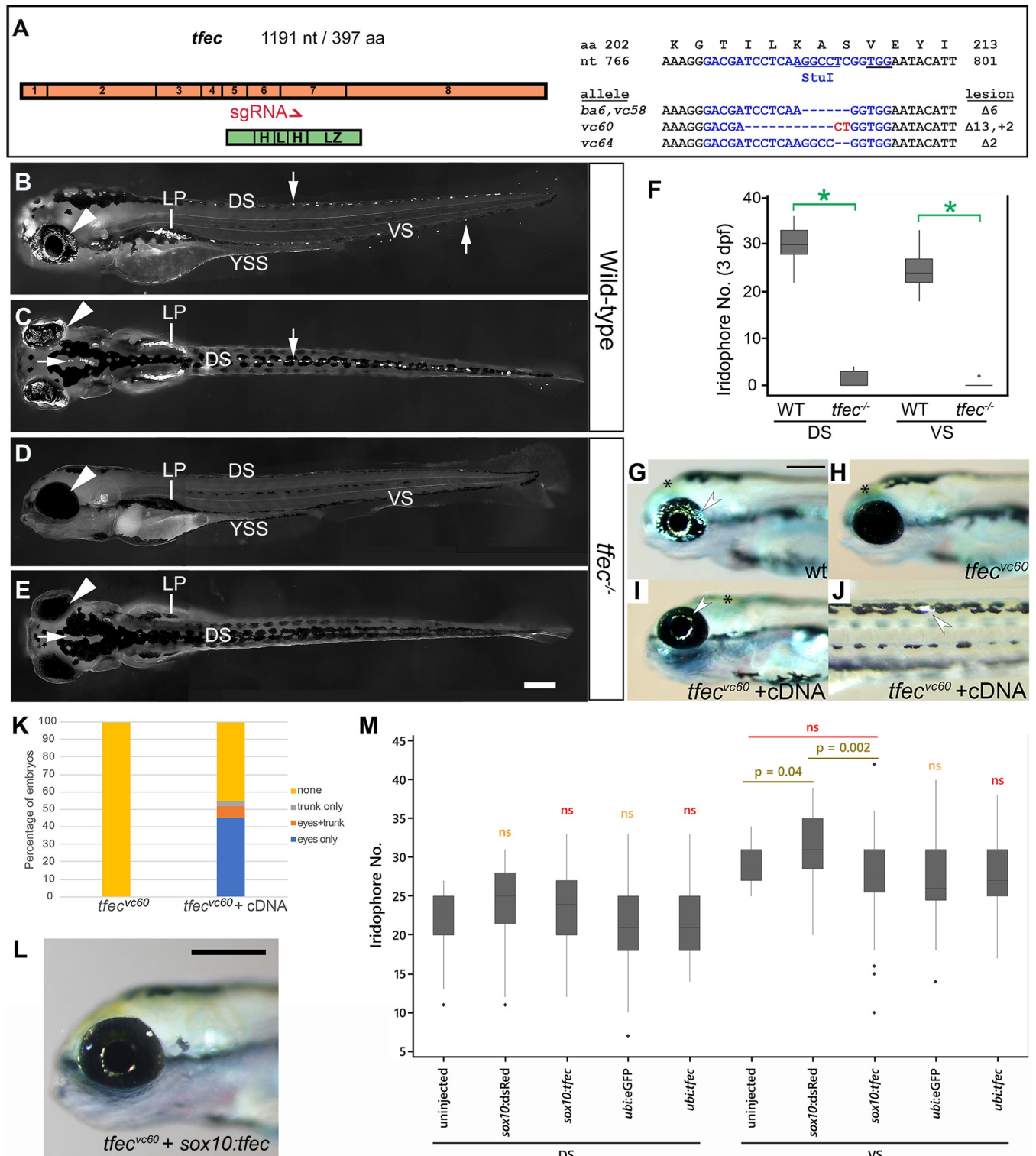


Fig 3. Loss of *tfec* function eliminates embryonic iridophores. (A) Schematic showing the distribution of the 8 exons of *tfec* (orange) in relation to the functional basic helix-loop-helix-leucine zipper domains (green) of the transcription factor. The red arrow indicates the position along both the gene and protein sequences targeted for mutagenesis by the CRISPR/Cas9 system. Included are the targeted WT *tfec* DNA/amino acid sequence (blue, with PAM underlined), and the sequences of the examined mutant alleles, with the corresponding molecular lesions (dashes for deleted nucleotides, red font for insertions). Imaging live embryos under reflected light reveals a striking lack of iridophores in *tfec* mutants (D,E) compared to their WT siblings (B,C) along the dorsal (downward arrow), ventral (upward arrow), and yolk sac stripes, as well as overlying the eye (arrowhead). Iridophores are also absent on the dorsal

head (C,E, horizontal arrow) and the lateral patches. (F) Quantitation of differentiated iridophores across the dorsal and ventral trunk at 3 dpf confirms a prominent lack of iridophores along the dorsal and ventral stripe of *tfec* mutants. (G-K) Injection of *tfec* cDNA can rescue the mutant phenotype. Differentiated iridophores (arrowheads) are abundant on the eye of WT embryos (G), but completely absent from the eye of a *tfec*^{vc60} mutant sibling (H) at 4 dpf. Co-injection with Tol2 transposase of a construct where the *tfec* promoter drives transcription of the *tfec* cDNA sequence, leads to rescue of iridophores (arrowheads) on the eye (I) and trunk (J) of *tfec*^{vc60} mutants. (K) Quantitation of rescue efficiency. Approximately 45% of mutants displayed eye iridophore rescue, 3% showed rescue in the trunk only and 6% showed rescue both in the eyes and trunk (n = 62). By contrast, iridophores were never observed in uninjected *tfec*^{vc60} sibling larvae (n = 58). (L) *tfec* cDNA expressed from the *sox10* promoter is capable of rescuing iridophores (arrowheads) in *tfec*^{vc60} mutants by 4 dpf. (M) At 3 dpf, numbers of iridophores in the dorsal stripe (DS) of wild-type embryos does not significantly change between uninjected embryos and embryos injected with either of the control constructs (*sox10:dsRed*, *ubi:eGFP*; orange “ns”). Embryos injected with *sox10:tfec* or with *ubi:tfec* show no significant change in DS iridophore numbers compared to both uninjected, and control injected siblings (*sox10:dsRed*, *ubi:eGFP*, respectively; red “ns”). In the ventral stripe (VS), injection of the *ubi:tfec* construct led to no significant iridophore number alterations, when compared to both control-injected and uninjected siblings (red “ns”). *ubi:eGFP*-injected controls do not show differences in VS iridophores when compared to uninjected controls (orange “ns”). When injecting *sox10:dsRed*, a weakly significant increase in VS iridophores is observed (p = 0.04). *sox10:tfec* injection does not lead to significant changes compared to uninjected controls, but appears to lead to a decrease in numbers when compared to *sox10:dsRed* (p = 0.002). Dots indicate outliers. sgRNA, small guide RNA; DS, dorsal stripe; VS, ventral stripe; LP, lateral patches; YSS, yolk sac stripe. (B,D, G-J,L): lateral views. (C,E): dorsal views. Head towards the left. Scale bars: 200 μm. (F): spots signify outlier values *, p-value < 10⁻⁹ using t-test.

<https://doi.org/10.1371/journal.pone.0244794.g003>

siblings (S1 Table). The iridophore phenotype could be successfully rescued via injection of a Tol2 transposon-based plasmid containing 2.4 kb of the *tfec* promoter [42], guiding tissue-specific expression of full-length *tfec* (Fig 3G–3K). Although the WT number of iridophores was not recovered, almost half of the injected mutant embryos presented with rescue of iridophores either on the eye, the trunk, or both of those domains (Fig 3K). Moreover, successful iridophore rescue was further visible in injected fish raised to adulthood (S1D Fig). Rescue could also be achieved by *tfec* expression in NC progenitors using the *sox10* promoter (Fig 3L). In WT embryos, overexpression using either the *sox10* or the *ubiquitin B (ubi)* promoter did not lead to a significant increase of iridophore numbers (S3M Fig). In these results, only iridophore numbers in the ventral stripe showed a statistically significant difference when comparing injected *sox10:tfec* and *sox10:dsRed* controls, which we attribute to a likely biologically irrelevant increase in the cell numbers of *sox10:dsRed* control-injected compared to uninjected embryos. Supporting our conclusion that these alterations are not biologically meaningful, we detect changes neither in the number of ventral stripe iridophores between *sox10:tfec*-injected and uninjected embryos, nor in *ubi:tfec*-injected embryos.

Curiously, we found that ectopic expression of *tfec* in wild-type embryos using the *ubi* promoter led to increased numbers of melanised cells rather than iridophores as might have been expected (Fig 4A and 4B). This led us to explore whether *tfec* expression would rescue the melanocyte phenotype of *mitfa* mutants. Intriguingly, *tfec* expressed from either the *sox10* or *ubi* promoters was capable of rescuing melanocytes in *mitfa* mutants, in a manner qualitatively comparable to *sox10* promoter-driven *mitfa* (Fig 4C–4F).

In previous work, we showed that *tfec* is present in multipotent premigratory NCCs, which do not yet express definitive pigment cell markers (early NCCs, early Cbls; [14]). We further demonstrated that during early stages of specification and migration of NC derivatives, *tfec* expression transiently overlaps with that of *mitfa* in specified, but not definitive, iridoblasts (Ib (sp)). Here we report that melanogenesis is delayed in 30 hpf homozygous *tfec* mutant embryos when compared to WT or heterozygous siblings, supporting a functional role for Tfec during its transient expression in melanoblasts. Specifically, we observed a significant reduction in the numbers of differentiating melanocytes along the dorsal trunk, and the medial and lateral migration pathways (Fig 4G–4I and S1 Table). Melanocyte development recovers, and by 4 dpf mutant embryos present with the same number of melanised cells along their trunk as their WT or heterozygous siblings (Fig 4J–4L and S1 Table). To test whether this recovery resulted from stimulation of a regeneration response through activation of adult melanocyte stem cells, we asked whether it occurred in mutant embryos even when formation of these stem cells has been inhibited by treatment with the ErbB signaling inhibitor, AG1478

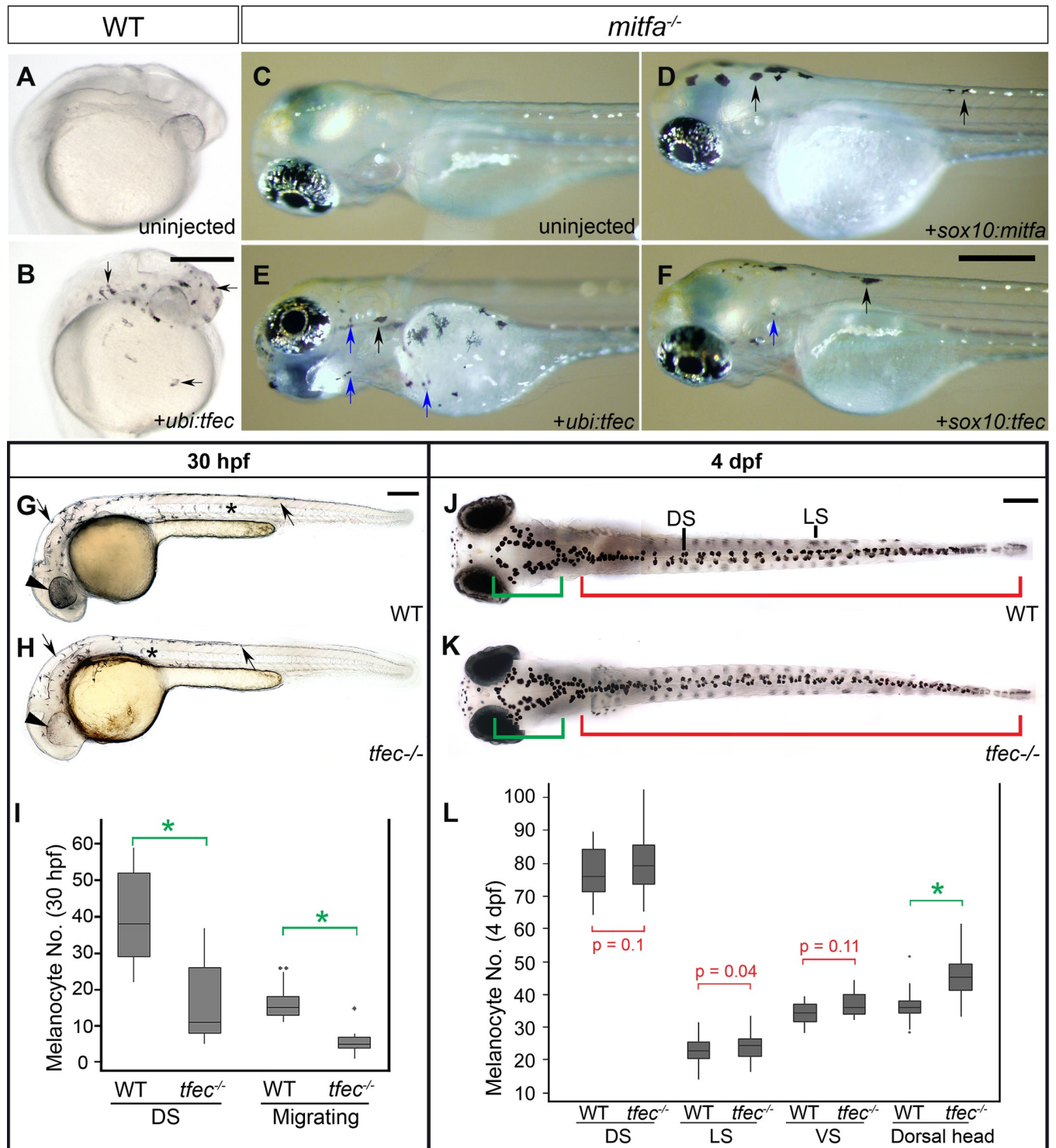


Fig 4. *tfec* can drive ectopic melanogenesis, and functions in the early stages of melanocyte development. (A,B) *tfec* cDNA expressed from the ubiquitin promoter induces ectopic melanisation in wild-type embryos by 24 hpf. (C-F) Shown at 72 hpf, *tfec* expressed from either the *ubi* or *sox10* promoters (E,F) rescues large well-differentiated melanocytes (black arrows) in *mitfa*^{w2/w2} embryos, in a manner reminiscent of *sox10*-driven *mitfa* (D), as well as apparently smaller, poorly melanised cells (blue arrows) (E,F). (G-I) Pigment cell phenotypes at 30 hpf. Compared to WT siblings (G), *tfec* mutants (H) have reduced melanisation of the RPE (arrowheads), and reduced melanocytes both along the dorsal trunk (arrows) and on the migratory pathways (asterisks). (I) Quantitation of melanocytes along the dorsal trunk and migratory pathways at 30 hpf reveals a 60% reduction in both regions in *tfec* mutants with respect to WT siblings. (J-L) Pigment cell phenotypes at 4 dpf. In embryos treated with melanin-concentrating hormone (MCH) to facilitate their quantitation, the

number of trunk and tail melanocytes is not significantly altered along the dorsal, ventral or lateral stripes (J,K, red region; quantitated in L), however there is a statistically significant increase in the number of melanocytes located on the dorsal head (J,K, green region; quantitated in L). Scale bars: (A-F), 250 μm ; (G,H,J,K), 200 μm . (I,L): spots signify outlier values; *, p-value < 10^{-9} using t-test.

<https://doi.org/10.1371/journal.pone.0244794.g004>

[43, 44]. Interestingly, melanocyte recovery was not affected by AG1478 treatment, indicating that the recovered melanocytes derive from embryonic NCCs, not from adult melanocyte stem cells (S2 Fig). Furthermore, we see strikingly reduced melanisation of the RPE of homozygous mutant embryos at 30 hpf, compared to WT or heterozygous siblings (Fig 3B and 3C), suggesting an analogous role in these brain (not NC)-derived melanocytes. Surprisingly, we observed a mild, yet consistent and statistically significant increase in differentiated melanocytes on the dorsal head of mutant embryos at 4 dpf (Fig 3D, 3E and 3L and S1 Table).

We set out to investigate the early specification events that lead to the observed pigmentation phenotypes by studying expression of iridophore markers. In homozygous *tfec* mutants, expression of the differentiated iridophore marker, *pnp4a* [14, 17], was largely undetectable at 48 hpf (Figs 5E and 5F and S3), consistent with complete lack of differentiated iridophores in *tfec* mutants. At both 24 hpf and 30 hpf, *pnp4a* was expressed in a notably reduced number of cells along the dorsal trunk, the migratory pathways and overlying the eye (Fig 5A–5D). Maintenance of *pnp4a* in a small subset of cells at these earlier stages of chromatoblast specification was attributed to *Mitfa*-dependent activation ([14]; Fig 5A–5D). Notably, the early reduction of *pnp4a* expressing cells in the eye and trunk of homozygous *tfec* mutants is consistent with a defect in generating the *pnp4a*⁺ Ib(sp) in these embryos. We assessed expression of *tfec* itself in *tfec* mutant embryos, using our *tfec*^{ba6} allele. At 24 hpf, presumptive homozygous mutants maintained *tfec* expression along the premigratory NC domain, even in anterior regions, indicating failure of a subset of NC derivatives to become fate specified, since in WT embryos fate specification to non-iridoblast fates is accompanied by loss of *tfec* expression in the majority of derivatives (Fig 5G and 5H). Furthermore, *tfec* expression was undetectable in the medial migration pathway, consistent with the absence of *tfec*-positive Ib(sp). At 36 hpf, the number of *tfec*-positive cells identified as Ib(df) [14] was strongly reduced in *tfec* mutant embryos compared to their siblings (Fig 5I and 5J), consistent with *tfec* function being fundamental for iridophore specification. Intriguingly, complete lack of differentiated iridophores (Fig 3B–3E) was not accompanied by corresponding total elimination of *tfec* expression at 48 hpf (Figs 5K and 5L and S3; [14]). As the remaining *tfec*-positive cells do not express other iridophore markers, such as *pnp4a* (Fig 5F) or *ltk* [14], we hypothesise that these correspond to early partially-restricted NC derivatives, perhaps early Cbls. Finally, we examine *ltk* expression in *tfec* mutants. *ltk* expression was completely lacking on the medial migration pathway in homozygous mutants at 24 hpf (Fig 5S and 5T; [14]), consistent with an early defect in iridophore specification. However, we note that *ltk* expression is also missing in the premigratory Cbl domain, indicating a much earlier role for Tfec, in specification of the Cbl(late) from Cbl(early).

The delayed melanogenesis phenotype in these mutants might result from delayed specification of melanoblasts, or from slowed differentiation of normally specified melanoblasts. To distinguish between these two possibilities, we performed chromogenic *in situ* hybridisation at 24, 30 and 48 hpf to detect expression of the melanocyte master regulator, *mitfa*. Strikingly, *mitfa* expression was restricted to premigratory late Cbls in *tfec* mutants, whereas *mitfa*-positive melanoblasts occupied the medial and lateral migratory pathways in WT and heterozygous siblings (Fig 5M and 5N). At 30 hpf, the delay was still detectable. The trunk was occupied by a relatively small number of *mitfa*-positive NC derivatives, whereas in the tail of mutants cells had still not entered the migratory pathways (Fig 5O and 5P). Consistent with the live phenotype, *mitfa* expression in mature melanocytes at 48 hpf was unaffected in the trunk and tail of

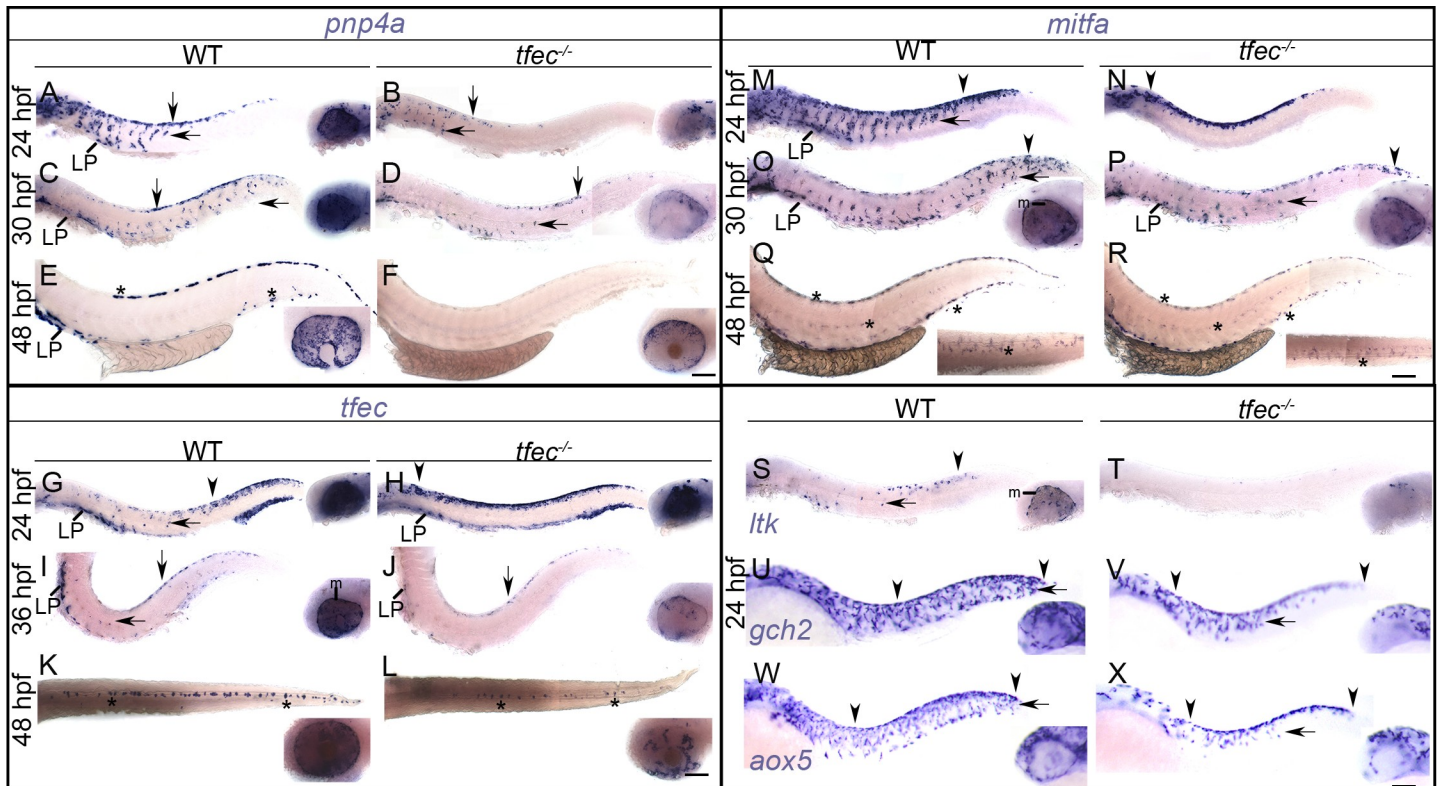


Fig 5. Specification of melanocytes, iridophores and xanthophores is delayed in *tfec* mutants. (A-F) *pnp4a* expression in Ib(sp) requires Tfec. At 24 hpf, the number of dorsally located, and of partially fate restricted, migrating chromatoblasts (arrows) expressing *pnp4a* is reduced in *tfec* mutants (A,B). Expression overlying the eye is also affected (A,B, insets). This reduction is still prominent at 30 hpf (C,D), when staining is also visibly affected in the lateral patches. *pnp4a* expression is undetectable in differentiated iridophore positions (E, asterisks) in *tfec* mutants at 48 hpf (F). *pnp4a*⁺ iridophore lineage cells overlying the RPE are noticeably reduced in *tfec* mutants compared to WT siblings (A-F, insets). (G-L) Generation of *tfec*-positive Ib(sp) from late Cbls requires Tfec. At 24 hpf, *tfec* mutants present with anterior expansion of the *tfec*⁺ premigratory NC domain (G,H, arrowheads) and lack of medially migrating, Ib(sp) progenitors (arrows). At 36 hpf, the number of dorsal and migrating *tfec*⁺ Ib(df) (arrows), as well as those located in the lateral patches is reduced in mutants, compared to WT or heterozygous siblings (I,J). At 48 hpf, a reduced number of cells (asterisks) express *tfec* along the dorsal stripe of mutant embryos, compared to WT or heterozygous siblings (K,L). *tfec* mutant embryos were distinguishable after whole-mount *in situ* hybridisation by the lack of RPE melanisation (I-L, insets). *tfec*⁺ iridophore lineage cells overlying the RPE are noticeably reduced in *tfec* mutants compared to WT siblings (G-L, insets). (M-R) Mb(sp) generation from the late Cbl is delayed in *tfec* mutants. At 24 hpf, *mitfa* marker expression is restricted to an increased number of premigratory Cbls (arrowheads) and is undetectable in migrating Mb(sp) (arrows) in *tfec* mutants (M,N). At 30 hpf, the numbers and distributions of *mitfa*-positive late Cbls (arrowheads) are indistinguishable between *tfec* mutants and WT or heterozygous siblings (O,P), but the delay in Mb(sp) migration (arrows) remains distinguishable towards the tail. *tfec* mutant embryos lack RPE melanisation (O,P, insets). At 48 hpf, *mitfa* expression in mature melanocytes (asterisks) is indistinguishable between *tfec* mutants and WT or heterozygous siblings (Q,R). (S, T) *tfec* mutants lack *ltk* expression in premigratory late Cbls (arrowhead), in migrating Ib(sp) (arrow) and in iridoblasts of the eye (insets). (U-X) Xanthoblast (Xbl(sp)) specification from Cbls is delayed, as indicated by examinations of two lineage markers, *gch2* (U,V) and *aox5* (W,X). At 24 hpf, laterally migrating Xbl(sp) (arrows) are restricted to more anterior regions and precursors located in the head are reduced in *tfec* mutants (V,X) compared to their WT siblings (U,W). All *tfec* mutant panels show the *tfec*^{bat6} allele except (V,X) which show the *tfec*^{vc60} allele. LP, lateral patches; m, melanisation. (A-J, M-X): lateral views. (K-L, insets of Q-R): dorsal views. Head towards the left. Scale bars: 100 μ m.

<https://doi.org/10.1371/journal.pone.0244794.g005>

tfec mutants, compared to WT siblings (Fig 5Q and 5R). This early retardation of *mitfa* expression, coupled to absence of *ltk* expression (Fig 5S and 5T; [14]), suggested that specification of the *mitfa*⁺; *tfec*⁺ Ib(sp) [14] from late Cbl, was hindered in the absence of functional Tfec. In addition, these data support our previous suggestion [14] that these Ib(sp) retain melanocyte potential (i.e. they can be considered both specified melanoblasts as well as specified iridoblasts), and show that melanocyte fate specification is delayed in the *tfec* mutant. The subsequent recovery of normal melanocyte numbers makes clear that compensatory factors allow melanoblasts to be specified, albeit with a short delay.

The *tfec* mutant embryos did not show obvious changes in the number and distribution of mature xanthophores (Fig 3G and 3H). However, examination of early xanthophore

specification markers by whole-mount *in situ* hybridisation showed that the developmental delay in producing melanoblasts is also true for generation of xanthoblasts (Fig 5U–5X). Specifically, both *aox5*- and *gch2*-positive cells appeared less abundant along the lateral migration pathway at 24 hpf. Delay in the expression of these two genes was also noted in the head of *tfec* mutant embryos, compared to WT siblings (Fig 5U–5X, insets). In conclusion, generation of melanoblasts, iridoblasts and xanthoblasts from multipotent NCCs is delayed in the absence of functional Tfec, pointing to an unexpectedly wide role in the specification of all chromatophore fates.

Loss of *tfec* function does not affect the development of non-pigment NC derivatives

Given the unexpected role in non-iridophore pigment cells, we then asked whether loss of *tfec* function affected non-pigment NC derivatives. To examine neural fates, we used a series of standard markers. The number and distribution of dorsal root ganglion (DRG) sensory neurons, as labelled by anti-Hu immunofluorescence, was unaffected by loss of *tfec* function (Fig 6A and 6B). Both our anti-Hu assays and traditional *in situ* hybridisation staining for *phox2b* expression (Fig 6C and 6D) indicated that development of the NC-derived enteric neurons and enteric and sympathetic progenitor cells remained unaffected in the absence of functional Tfec. Moreover, the number and patterning both of mature Schwann cells, normally residing on the posterior lateral line nerve along the horizontal myoseptum, and of satellite glial cells associated with the DRGs, remain unaffected in homozygous *tfec* mutants, as shown by staining for *sox10* at 48 hpf (Fig 6E and 6F). Likewise, developing oligodendrocytes in the CNS appear unaffected in their numbers and distribution.

To examine whether specification of neural derivatives from multipotent progenitors is delayed in *tfec* mutants, similar to non-iridophore pigment cell derivatives, we conducted additional whole-mount *in situ* hybridisation experiments between 30 hpf and 48 hpf, when relevant early specification markers are detectable. We found that expression of *pou3f1* (previously *oct6*) in migrating precursors of the posterior lateral line nerve (pLLn) appeared normal in *tfec* mutants, compared to known WT siblings (Fig 6G and 6H). Furthermore, detection of *sox10* expression in batches containing WT, heterozygous and *tfec* mutant embryos failed to detect alterations in either the distribution or the abundance of glial progenitors migrating along the medial pathway (Fig 6I and 6J). These *in situs* provide evidence that premigratory NCCs appear to be present in normal numbers and show unaltered timing of downregulation of *sox10* expression. In assays aiming to detect *sox10* transcript at 30 hpf, we were able to confirm the presence of homozygous mutant embryos based on reduced melanisation of the RPE (Fig 6I and 6J, insets).

We then asked whether ectomesenchymal derivatives were affected in *tfec* mutants. We performed *in situ* hybridization at 30 hpf to detect *dlx2a* transcript in migrating cranial NCCs (Fig 6K and 6L), and found no visible differences in numbers or distributions of cells between WT and *tfec* homozygous mutant embryos. To assess cartilage deposition, we stained *tfec* mutant embryos and WT siblings with Alcian Blue at 4 dpf, but did not note any phenotypic distinction in homozygous mutants (Fig 6M and 6N). For the aforementioned experiments, from 48 hpf onwards homozygous mutants, identified by their iridophore phenotypes, were processed separately from their siblings (Fig 6A–6D, 6M and 6N).

In summary, although *tfec* expression is prominent in the majority of, if not all, early NCCs [14, 39], we could not detect any changes at any stage of the development of NC-derived neurons, glial cells and skeletal components. This suggests that although *tfec* transcript is present at these early stages, Tfec is uniquely required for pigment cell fate specification, and essential for iridophore fate specification.

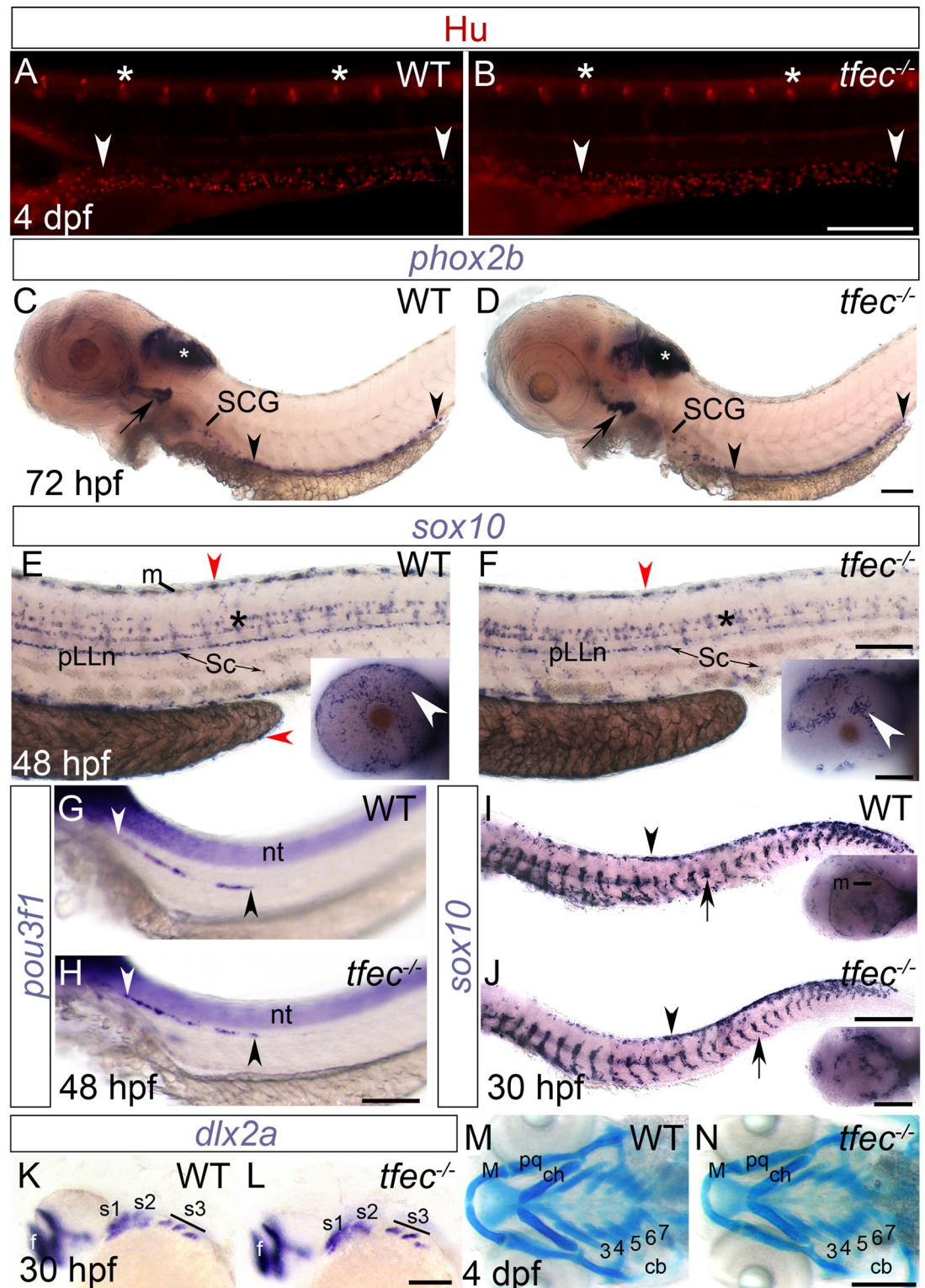


Fig 6. Development of skeletal and neural NC derivatives is unaffected in *tfec* mutants. (A–J) Peripheral nervous system derivatives develop normally in *tfec* mutants. (A,B) At 4 dpf, the DRG (asterisks) and enteric neurons (arrowheads) number and positioning, as revealed by immunofluorescent detection of Elav1/Hu, is indistinguishable between *tfec* mutant embryos (B) and WT siblings (A). (C,D) *phox2b* expression, detected by whole-mount *in situ* hybridisation, at 72 hpf. The formation and the extent of migration of enteric nervous system progenitors (region between arrowheads) are indistinguishable between *tfec*

mutants and WT siblings. Likewise, expression in the earliest differentiating region of the sympathetic ganglia chain, the superior cervical ganglion (SCG), is unaffected. *phox2b* expression is also indistinguishable in the hindbrain (white asterisks) and in placode-derived neuronal progenitors in the cranial ganglia associated with the branchial arches (arrows). (E,F) At 48 hpf, *sox10* expression analysis showed indistinguishable numbers and distribution of Schwann cells (Sc) occupying the pLLn and spinal nerves. Likewise, oligodendrocyte progenitors throughout the CNS appear normal in their specification, numbers and migration (asterisks). *sox10* expression is detectable in iridophore positions (red arrowheads) and in eye iridophores (insets, white arrows), that are strongly affected in homozygous *tfec* mutants. (G,H) *pou3f1* expression analyses at 48 hpf show that glial progenitors on the posterior lateral line nerve (pLLn; area between arrowheads) develop normally in *tfec* mutants. (I,J) *sox10* staining at 30 hpf indicates no observable alterations in the migration of specified neural progenitors through the medial pathway (arrows) in *tfec* mutants, compared to WT siblings. Likewise, the number and distribution of *sox10*-positive premigratory NC progenitors (arrowheads) is unaffected. *tfec* mutants were identified by lack of RPE melanisation (I,J, insets). (K,L) At 30 hpf, *dlx2a* expression shows that formation of the three streams (s1-s3) of migrating cranial NCCs is unaffected in *tfec* mutants. Staining is also indistinguishable in the forebrain (f). (M,N) The cranial cartilage at 4 dpf is unaffected in *tfec* mutants, versus WT siblings, as indicated by Alcian blue staining. Numbered 3–7 are the positions of the branchial arches. (B,H,L,N): *tfec^{inc60}* allele, (D,F,I): *tfec^{bas6}* allele. cb, ceratobranchials; ch, ceratohyal; M, Meckel's cartilage; nt, neural tube; pq, palatoquadrate. (A–L): lateral views. (M,N): dorsal views. Head towards the left. Scale bars: (A, B, G, H, K–N): 200 μ m; (C–F, I, J): 100 μ m.

<https://doi.org/10.1371/journal.pone.0244794.g006>

***tfec* is downstream of NC specifier genes in the NC progenitor GRN**

As indicated in Fig 1, *tfec* expression appears early in NCC development, within multipotent progenitors and coinciding with *sox10* and *foxd3*, likely just after *snai1b* and *sox9b* have been downregulated. To determine the upstream regulators of *tfec* in premigratory early NCCs and early Cbls of the dorsal trunk, we conducted expression studies on single and double mutants for the important vertebrate NC specifier genes *foxd3*, *sox9b*, *sox10* and *tfap2a* [41]. In these experiments, where we were using large sample sizes to ensure sufficient single and double mutant embryos, phenotypes associated with genotypes were identified using statistical testing of phenotypic ratios in comparison with expected Mendelian ratios; in the following discussion we refer to ‘presumed mutants’ in reference to their inferred genotype. The sample sizes and *p* values are detailed in S2 Table. Interestingly, at 18 hpf, all embryos from crosses of *foxd3*, *sox10* and *tfap2a* mutant carriers showed identical expression of *tfec*, strongly suggesting that early expression of *tfec* is not strictly dependent upon any one of these genes (S2 Table). In contrast, in 18 hpf presumed homozygous *sox9b* mutants, *tfec* expression does not extend towards the tail as far as in WT or heterozygous siblings (Fig 7K and 7L and S2 Table), which is likely attributable to delayed specification of early NCCs upon loss of *sox9b* function. At 24 hpf *tfec* expression in WT embryos is gradually downregulated from the majority of premigratory NCCs of the trunk in an anterior to posterior manner, strongly persisting only in Ib (sp) [14]. However, we observed a persistence of *tfec* expression in the anterior premigratory NC domain in *sox10*, *sox9b*, *tfap2a* and *foxd3* mutants at this stage, consistent with retained premigratory late Cbls (Fig 7A–7D and 7M–7N). This persistence differed in severity and duration between different mutants, but homozygous mutants of each genotype show highly consistent phenotypes across experimental replicates. Specifically, as was previously reported for a single time point [14], in *sox10* mutants, where NC derivatives fail to become specified and to enter the migration pathways [11, 20], *tfec* expression is maintained in trapped late Cbls, extending to the hindbrain/trunk boundary (Fig 7A and 7B). Our results show that, at all time-points, *tfec*-positive premigratory progenitors persist in homozygous mutants (identified by their lack of *tfec* expression in Ib(sp) positions), until 36 hpf (Fig 7A, 7B, 7E–7F and 7I–7J). In each of *sox9b*, *tfap2a* and *foxd3* homozygous mutants at 24 hpf, *tfec*+ premigratory NCCs are detectable along the dorsal trunk, but not reaching the hindbrain/trunk boundary as in *sox10* homozygous mutants (Figs 7C, 7D, 7N and S4).

As members of the same SoxE group, it is not surprising that *sox10* and *sox9b* have been shown to be functionally redundant in DRG sensory neuron development [22]. We asked whether this might also be true for *tfec* expression in early or late Cbls. Examination of embryo

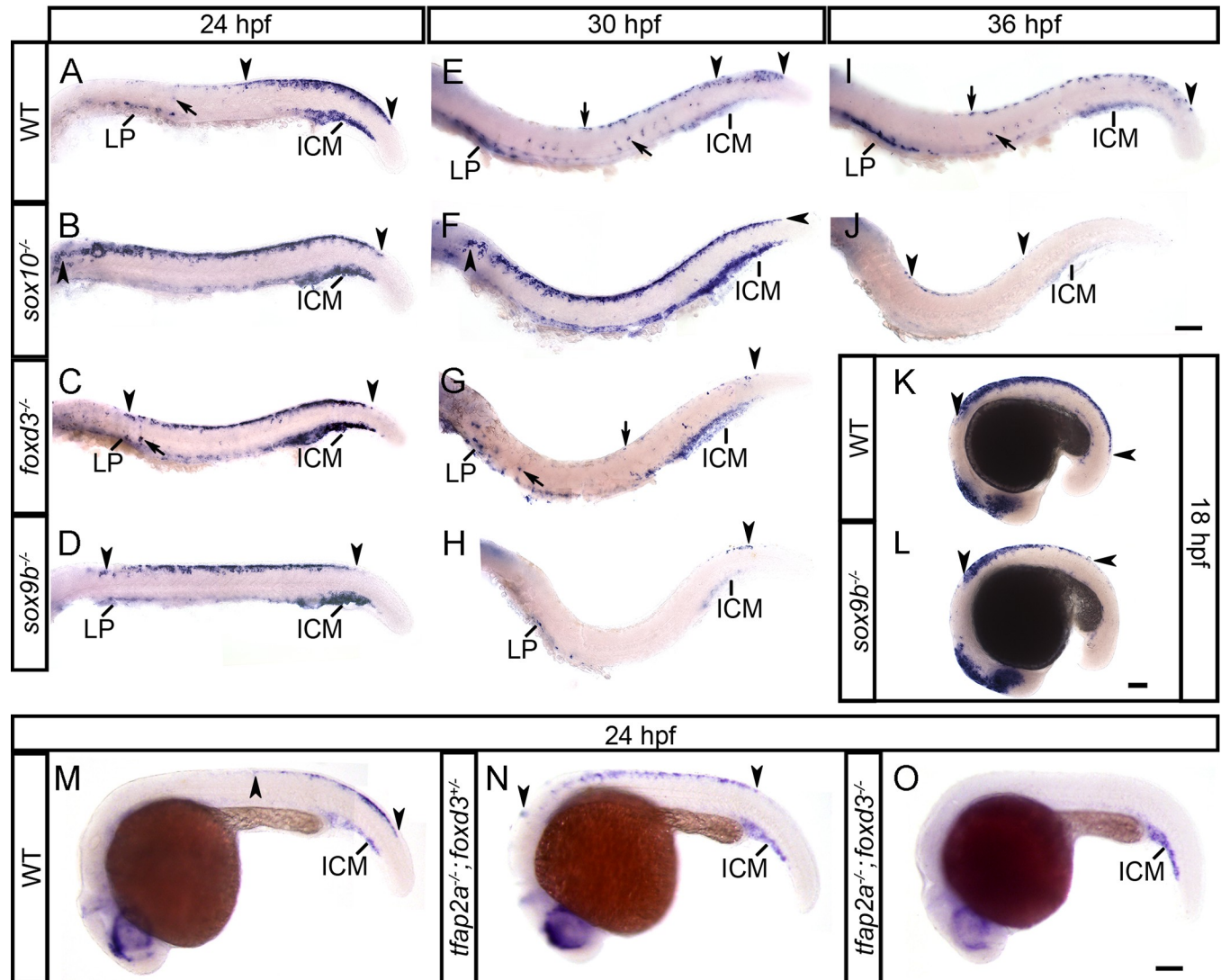


Fig 7. *tfec* is a member of the GRN functioning to specify multipotent NCCs, following their induction. In *sox10*, *foxd3* and *sox9b* mutants (B,C,D) at 24 hpf, *tfec*-positive late CbIs are trapped in the premigratory domain along the trunk, whereas in the WT (A) they are restricted to the dorsal tail (regions between arrowheads). Consistent with failed or delayed development of NC progenitors, migrating (arrow) and LP-located Ib(sp) (A) are reduced (C,D) or completely absent (B). The anterior expansion of the progenitor domain is more pronounced in *sox10* mutants (B). Initiation of expression in eNCCs, detected by posterior-most boundary of expression (posterior arrowhead), is normal in *sox10* (B) and *foxd3* (C) mutants, but is perceptibly delayed in *sox9b* mutants (D); this effect is also prominent at 18 hpf (L). In 30 hpf WT embryos (E) *tfec* transcript is detectable in premigratory late CbIs of the posterior tail (region within arrowheads). This domain still shows a dramatic expansion in *sox10* mutants (F, arrowheads), while *foxd3* (G) and *sox9b* (H) mutants no longer present with trapped progenitors. Instead, very few *tfec*⁺ cells are detectable in the dorsal tail (arrowheads), and there is a prominent reduction in Ib(df) (arrows, lateral patches). (I) In WT embryos at 36 hpf, *tfec* is still expressed in premigratory CbIs in the posterior-most tail (arrowhead), as well as Ib(df) (arrows). In *sox10* mutants (J) trapped premigratory progenitors (region within arrowheads) are reduced, but still visible. *tfec* expression in the premigratory NC domain (region within arrowheads) is anteriorly shifted in single *tfap2a* mutants (N), compared to WT siblings (M) at 24 hpf, but completely eliminated in double *tfap2a*;*foxd3* mutants (O). *tfec* expression is invariably detectable in the intermediate cell mass from 18 hpf to 36 hpf, in WT and mutant embryos (A-O). ICM, intermediate cell mass; LP, lateral patches. Lateral views, head towards the left. Scale bars: 100 μ m.

<https://doi.org/10.1371/journal.pone.0244794.g007>

batches containing *sox10*;*sox9b* double mutants at 18 hpf did not reveal elimination of *tfec* expression in any of the assessed embryos (S2 Table). However, *tfec* expression was completely eliminated from the NCC progenitor domain of genotyped *tfap2a*;*foxd3* double mutants (Fig 7M–7O), suggesting that both these genes act together to upregulate *tfec* expression in premigratory NCCs of the trunk. This effect was not observed in genotyped siblings, heterozygous

for one or both alleles nor those homozygous for a single mutant allele. In conclusion, our data show key, but redundant, roles for *foxd3* and *tfap2a* in establishing expression of *tfec* in premigratory multipotent NCCs.

Mitfa represses *tfec* during melanocyte development

Both *tfec* and the melanocyte master regulator, *mitfa*, are transiently expressed in the multipotent NCC domain, in late Cbls, as well as in Ib(sp). We conducted whole-mount *in situ* hybridisation to assess the effects of loss of *mitfa* function on *tfec* expression. Interestingly, presumed homozygous *mitfa* mutants show ectopic expression of *tfec* along the dorsal trunk and in NC derivatives along both the medial and lateral migration pathways (Fig 8A–8D). This pattern of *tfec* expression in *mitfa* mutants resembles WT *mitfa* expression in developing melanoblasts, therefore it is likely that Mitfa represses *tfec* expression in NCCs that become biased towards the melanocyte lineage. This effect persists at 30 hpf and is also observed by a complementary, and more sensitive fluorescent transcript detection technique, RNAscope; we see persistence of *tfec* expression in cells migrating through the lateral pathway (Fig 8E–8F'). These cells co-express the definitive lineage marker, *ltk* [11, 14], suggesting that they correspond to specified iridoblasts.

Discussion

Our previous work established *tfec* as a marker during NC development and iridophore fate choice [14, 39]. Interestingly, *tfec* was found to be co-expressed with *mitfa* in specified iridophore (Ib(sp)) cells, proposed to be able to at least give rise to melanocytes and iridophores, but not in mature melanocytes. Thus, Ib(sp) should also be considered as specified melanoblasts. The first aim of the present study was to determine whether iridophores are indeed the only embryonic differentiated pigment cell expressing *tfec*; to this end, we conducted analyses showing that *tfec* expression is maintained at detectable levels only in mature iridophores, but neither in melanocytes nor in xanthophores, in agreement with recently published single cell transcriptomics analyses [45].

Considering the strong sequence conservation between Tfec and the melanocyte master regulator, Mitfa, we next asked whether *tfec* might have a function in iridophores analogous to that of *mitfa* in melanocytes; i.e. as the master regulator of the iridophore lineage. We generated mutations in *tfec* using a CRISPR/Cas9 approach, obtaining several alleles which displayed essentially identical phenotypes. Although *tfec* mutants have been generated independently [46], that report did not examine NC-related defects, focusing instead on deficiencies in hematopoiesis. As with the CRISPR-generated exon 3 allele reported by Mahony and colleagues, our mutants fail to inflate the swim bladder (which, along with the caudal hematopoietic tissue, is another site of *tfec* expression; [39]) and die after approximately 12 days, apparently from lack of ability to feed. Potential postembryonic roles of *tfec* remain unclear. Nevertheless, data from mosaic adults and a single adult escaper suggest that *tfec* is required for iridophores throughout the lifetime of the animal (S1 Fig).

In order for *tfec* to be considered the iridophore master regulator, the gene must not only be necessary, but also sufficient for iridophore specification. Our loss of function data are strongly suggestive of *tfec* being required for iridophore development, as *mitfa* is for melanocytes (Fig 1). Injection of wild-type *tfec* cDNA under its own promoter could rescue, albeit only partially, the iridophore phenotype in *tfec* mutants, with rescued iridophores in the eye observed more often than in the trunk. These results show that Tfec is sufficient to rescue iridophore specification in *tfec* mutants. However, we show that addition of *tfec* failed to generate additional iridophores in wild-type fish. Our additional gain of function experiments in WT

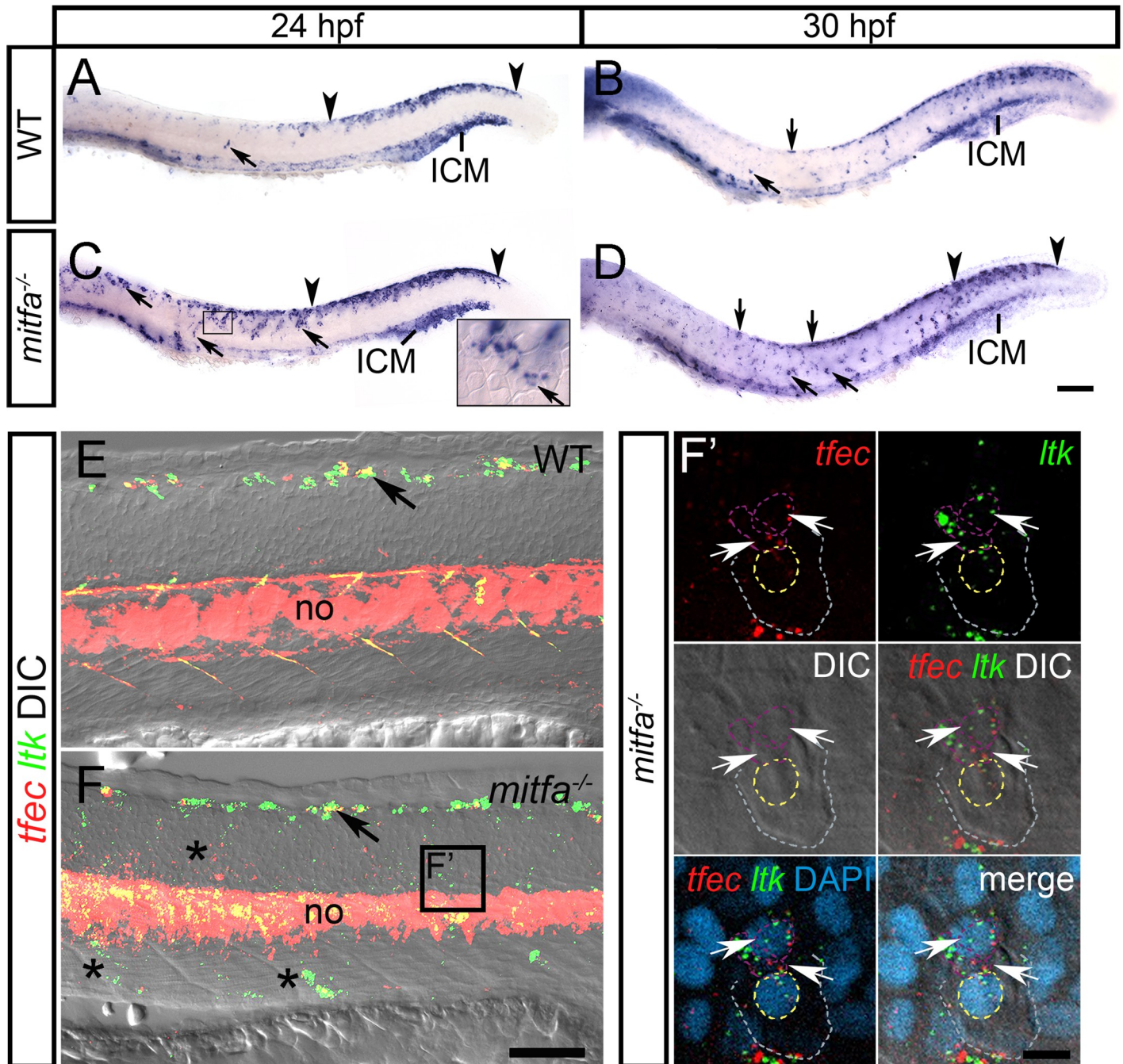


Fig 8. Mitfa represses *tfec* expression in melanoblasts. In WT embryos at 24 hpf (A) and at 30 hpf (B), *tfec* expression is detectable in Ib(sp) and Ib(df) (arrows), respectively, and in the posteriorly regressing early NCC/Cbl domain of the dorsal posterior trunk and tail (region within arrowheads), but expression is undetectable in the lateral migration pathway. At 24 hpf (C) and at 30 hpf (D), *mitfa* mutants present with an increased number of *tfec*-positive cells (arrows) along the dorsal trunk, as well as in the medial and lateral (C, inset) migratory pathways. RNAscope (E,F) performed on *mitfa* mutants at 30 hpf shows an increased number of *tfec*-positive cells compared to the WT on the migration pathways (F, asterisks). Arrows indicate iridoblast precursors along the dorsal trunk. (F') RNAscope reveals that in *mitfa* mutants ectopic *tfec*-positive cells migrating on the lateral migration pathway (below the epidermis; grey and yellow dashed lines indicate the periphery and nuclear boundary, respectively, of overlying keratinocytes) co-express *ltk* (arrows; nuclei indicated by purple dashed lines), and thus likely correspond to Ib(sp). ICM, intermediate cell mass; LP, lateral patches; no, notochord. Lateral views, head towards the left. Scale bars: A-D: 100 μ m; E,F: 50 μ m; F': 10 μ m.

<https://doi.org/10.1371/journal.pone.0244794.g008>

embryos suggest that the iridophore number is not altered upon supplementation of *tfec*, whether ubiquitously in the embryo using the *ubi* promoter, or specifically in NCCs using the

sox10 promoter. This indicates that either Tfec is insufficient to alone drive NSCs to adopt the iridophore fate, or that in wild-type embryos any elevated specification of the iridophore lineage is compensated by cell regulation mechanisms. Consistently, ectopically expressing Tfec in *mitfa* mutant embryos failed to increase the number of iridophores. Thus, our experiments to date are indicative of an additional, uncharacterised cofactor cooperating with Tfec to generate iridophores in zebrafish embryos, and without this cofactor, Tfec is not sufficient to promote iridophore specification. The immediate MiT family candidate, Mitfa, is excluded as a potential Tfec cofactor, as it is not essential for iridophore specification [17]. Single cell transcriptomics experiments will be important to indicate candidate transcriptional regulators that might form an iridophore master regulator complex together with Tfec. Further experiments will be required to determine if the mechanism by which Tfec functions in iridophore specification is analogous to that of Mitfa in melanocytes. For example, Mitfa is able to efficiently rescue melanocyte development in the absence of *sox10* through triggering both an Mitfa autoregulatory feedback loop and expression of melanocyte differentiation genes [13, 25]. We have shown a Tfec-dependent autoregulatory loop in iridophore development, which may explain why rescue of the iridophore phenotype in *tfec* mutants is very inefficient.

In addition to a complete absence of iridoblasts and mature iridophores our mutants also, surprisingly, presented with delayed differentiation of both NC-derived and RPE melanocytes, as well as of xanthophores. This suggests that Tfec has a subsidiary role in specification of each of the pigment cell-types. The melanocyte specification delay phenotype that we describe may also help explain the otherwise rather surprising observations of *tfec*-dependent melanocyte rescue upon inducing gain of function in homozygous *mitfa* mutants, suggesting that *tfec* can, when overexpressed, functionally substitute for *mitfa*. Work in mice has demonstrated at least partial functional redundancy between the two genes in the mammalian RPE [47] and a cooperative relationship between *mitfa* and *tfec* has also been recently indicated in the context of eye melanisation and choroid fissure closure [48]. Considered with these previous studies, our results suggest that MiT gene dosage may be an important factor in both neural crest and retinal pigment cells. The nature and origins of either the ectopic or the rescued melanocytes we describe here remain unclear. It is plausible that some, but clearly not all, of the ectopic melanised cells observed upon broad *tfec* overexpression (via the *ubi* promoter) may be of an RPE character, rather than neural crest melanocyte character. Transcriptomics analyses and detailed evaluation of the spatio-temporal requirements for melanocyte rescue, as well as Tfec-Mitfa protein-protein and DNA interactions, will be necessary to elucidate the origins of such cells, and the seemingly intricate relationship between Mitfa and Tfec during pigment cell development. Finally, work to define direct and indirect transcriptional targets of Tfec, as well as any other transcriptional co-regulators, similar to the role of Tfp2a for Mitfa [27], is needed to understand the mechanistic details of iridophore fate choice.

Nevertheless, we found that development of all non-pigmented derivatives (neurons, glia and skeletal components) is unaffected. This striking phenotype, with effects restricted to pigment cell specification, is unique amongst the characterised zebrafish pigment mutants and would be consistent with the hypothesis that the cell type defined by *tfec* expression is a fate-restricted tripotent precursor of the three chromatophore lineages. Decades ago, it was proposed that melanocytes share a common origin with iridophores and xanthophores from a pigment-restricted precursor [15], which we would term a chromatoblast (Cbl(late)). More recently, analysis of *ltk* expression in *sox10* mutants indicated the presence of an *ltk*⁺ precursor of pigment cells, consistent with the chromatoblast [11]. The *tfec* loss of function phenotype thus provides further support for the existence of a Cbl, transiently localised within the dorsal trunk of embryos between 18 hpf and 24 hpf ([14]; Fig 9).

In a recent single cell lineage tracing study, Singh et al., identified progenitor cells proposed to generate all 3 pigment cell types throughout embryogenesis and into adulthood. However, it was shown that the vast majority of these were also able to give rise to neuronal and glial lineages [12]. These results strongly argue for the absence of a strictly tripotent progenitor (Cbl(late)) in each of the 3 embryonic and 1 adult stages when the studies were conducted; but the hypothesis that a transient Cbl(late) cell exists during a brief time window (between 18 hpf and 24 hpf) cannot be strictly ruled out. An alternative hypothesis would be that, although *tfec* is expressed in a more widely multipotent progenitor (Cbl(early)), its function is only required for downstream specification of chromatophores. Such a hypothesis is further supported both by ours and others' data on embryonic *tfec* expression, which is detected across the entire premigratory domain of multipotent NCCs [14, 45]. Based on our findings, *tfec* is the first zebrafish gene identified that specifically affects all chromatophore lineages without appearing to affect any non-pigment NC derivatives. The key NC transcriptional regulator, *sox10*, is required for each of the three pigment cell lineages, but loss of *sox10* function additionally results in strong reductions or absence of all peripheral glia cells and NC-derived peripheral neurons, suggesting that neuronal and pigment lineages share a common, non-ectomesenchymal progenitor [19]. Furthermore, this requirement of pigment cells for *sox10* manifests itself apparently in different ways; *sox10* is required for *mitfa* expression in late Cbls, and *mitfa* can promote melanocyte fate in the absence of *sox10* if misexpressed [25]. In contrast, *sox10* mutants still strongly express *tfec* (as well as *ltk*) within trapped premigratory progenitors, yet fail to produce Ib(sp) [14]. We show here that in *tfec* mutants the ability to express the lineage markers of melanocytes and xanthophores is delayed but otherwise unaffected, whereas *ltk* expression is completely missing, even in premigratory cells, also contrasting the phenotype of *sox10* mutants [11]. Thus, Tfec is necessary for both correct and timely chromatoblast specification, either via generation of a tripotent progenitor (Cbl(late)) and/or through independent roles in each chromatophore lineage arising from a multipotent progenitor (Cbl(early)).

Another aim of the work presented here was to extend the GRN surrounding *tfec* beyond the iridophore lineage by examining its regulation in early NCCs [14, 39]. Initiation of *tfec* expression in the early NC is not affected by loss of *tfap2a*, *foxd3* nor *sox10* alone. Notably, loss of *sox9b* alone caused an apparent delay in induction of *tfec* expression in posterior NC yet, despite this alteration in the pattern, expression remained strongly present in the progenitor population.

Sox10 and Sox9b have previously been reported to act redundantly during zebrafish development [13, 22]. Our data, however, demonstrates that *tfec* expression in double *sox10;sox9b* mutant embryos is still strongly activated in the NC. It remains to be shown whether loss of function of a single or of both *sox10* alleles modifies the degree of *tfec* expression delay noted in homozygous *sox9b* mutants.

Double mutants for *tfap2a;foxd3* have been shown to eliminate induction of NC [52]. Redundant activities of Tfap2a and Tfap2c are required for NC induction and development of other non-neural ectoderm derivatives in zebrafish embryos [52, 53]. Consistent with this, we found that *foxd3* and *tfap2a* are redundantly required for induction of *tfec* expression in early premigratory NCCs (Fig 9B). In this context, it is interesting that *tfec* was recently identified as a likely direct target of Tfap2a/2c, through analysis of gene expression changes in mutants combining different numbers of *tfap2a* and *tfap2c* mutant alleles [54]. The same study demonstrated the functional compensation of Tfap2a by Tfap2c, since in *tfap2a* mutants just a single copy of *tfap2c* was sufficient to maintain *tfec* expression at WT levels and rescue NC specification. Our data support the above finding, showing that transcriptional regulation of *tfec* via Tfap2 transcription factors is independent of them first activating *sox10* or *sox9b* [49–51] (Fig 9B). Moreover, our assays indicate that disruption of Foxd3 activity alongside Tfap2a

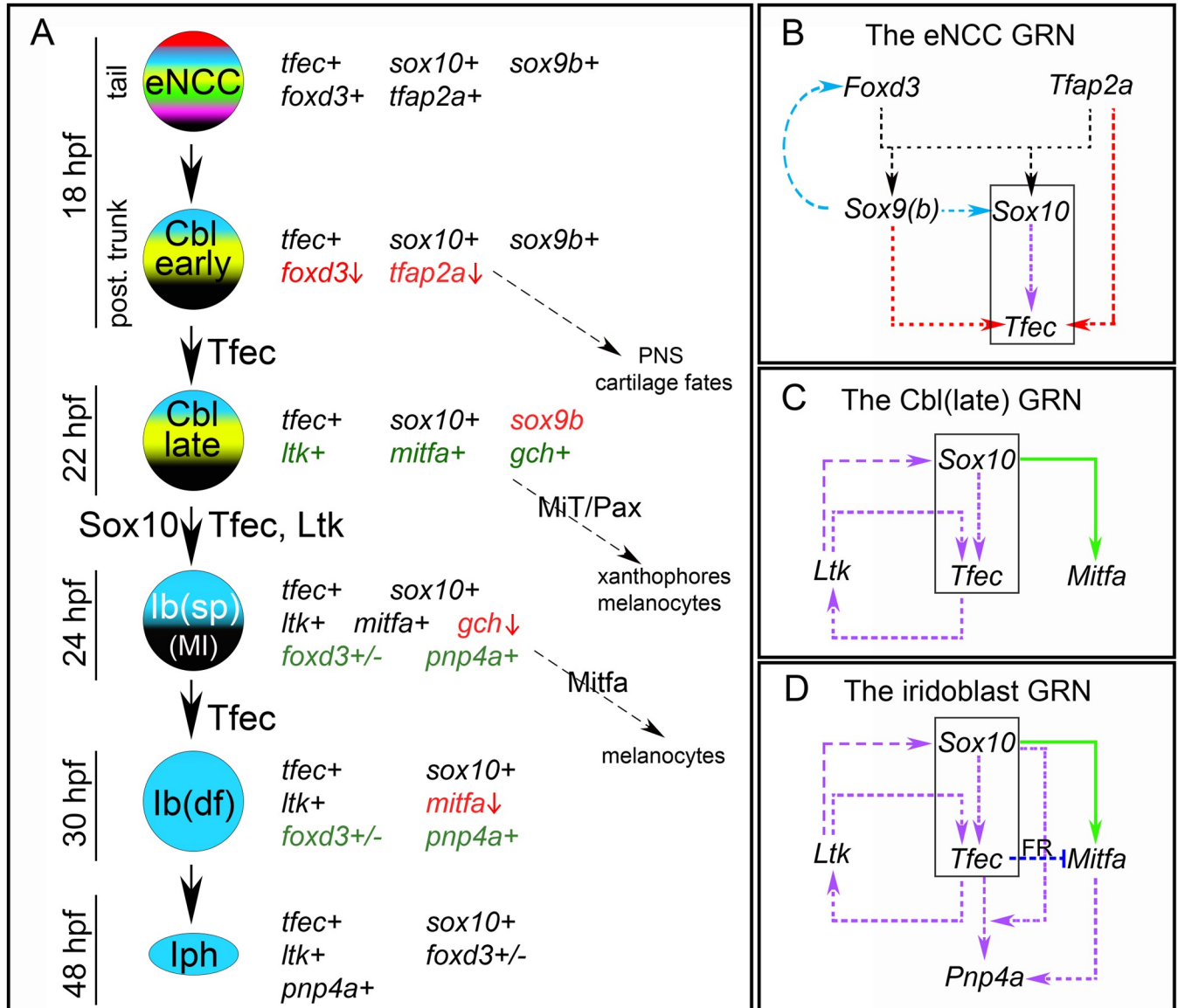


Fig 9. *tfec* is broadly expressed during progressive fate restriction of the iridophore lineage from eNCCs, and is required to specify definitive iridoblast, Ib(df), from the melano-iridoblast, Ib(sp). (A) Schematic representation of partially restricted iridophore progenitors during development, along with the expression characteristics and potential fate choices of each ([14], this work). *tfec* is initially co-expressed with eNCC specification factors, which gradually become downregulated (red font, vertical red arrow), while lineage-specific factors become upregulated (green font). Proteins indicated on the black arrows are considered important for the respective fate restriction step. (B) The position of *tfec* in the GRN guiding vertebrate NCC induction. Dashed arrows indicate interactions which could be either direct or indirect. In multipotent NCCs, Tfp2a and Foxd3 redundantly activate *tfec* expression (red arrows; this work), which is later maintained in the iridophore lineage by Sox10 (purple arrow; [14]). This activation occurs independently of previously described co-regulation of zebrafish *sox9b* and *sox10* expression by Tfp2a and Foxd3 (black arrows; [49]), and is unaffected by potentially conserved activation of *sox10* and *foxd3* by Sox9b (blue arrows, as shown in chick; [50, 51]). (C) Following transition of Cbl early to Cbl late, *tfec* expression is supported by positive feedback interactions between Sox10, Ltk and Tfec, as described in Petratou et al., 2018 [14]. Sox10 directly activates *mitfa* expression (solid green arrow; [25]), which during early Cbl specification is co-expressed with *tfec* [14], inhibiting its expression to bias progenitors towards the melanocyte fate. (D) As the lineage progresses past the Cbl, into the Ib(sp), Ib(df) and mature iridophore stages, factor R (FR) mediates Tfec-dependent downregulation of *Mitfa* (dark blue edge), and expression of the marker *pnp4a* becomes prominent [14]. In (B-D) the black box outlines the core connecting the three networks. MiT, microphthalmia family transcription factors; PNS, peripheral nervous system.

<https://doi.org/10.1371/journal.pone.0244794.g009>

counteracts functional compensation by Tfp2c. Further work will be required to assess whether this is due to a role for Foxd3 in Tfp2c expression.

Our data formally establish *tfec* as a member of the GRN governing maintenance of NCC progenitors [41]. Furthermore, our data provide the first evidence for Tfec function in those early progenitors, since we show it is required to drive early expression of *ltk* at the Cbl stage, as well as fate specification of the iridophore lineage from these multipotent progenitors.

Although *tfap2a* and *foxd3* act redundantly to activate *tfec* expression in early NCCs, they also present with divergent ongoing effects in pigment lineages. Single mutations in *tfap2a* and *foxd3* affect the melanocyte and iridophore lineages, respectively [28, 29, 55], likely in a manner dependent upon distinct regulatory interactions with Mitfa. While *tfap2a* and *mitfa* work in parallel to promote melanocyte differentiation [27], *foxd3* has been suggested to repress *mitfa* transcription [16, 56], at least in some contexts [14]. In the absence of *foxd3*, iridophore numbers are reduced in a manner that is at least partially *mitfa*-dependent, and marker analyses and lineage-tracing experiments support the existence of a bipotent melanocyte-iridophore (MI) precursor, the fate of which is influenced by this *foxd3/mitfa* interaction [12, 17]. Our findings that *mitfa* represses *tfec* expression in melanoblasts, and that *tfec* mutants have increased melanocytes, indicate that maintenance of *tfec* activity is also key to the melanocyte versus iridophore cell fate decision. Notably, Mitfa and Tfec have the potential to physically interact as a heterodimer [57, 58], which adds an additional layer of complexity when attempting to elucidate the mechanism of cell fate choice. Interestingly, despite the similarity between *tfec* and *ltk* mutant iridophore phenotypes, *ltk* mutants do not show an analogous late increase in melanocytes [11].

Specification and differentiation of the third pigment cell type of zebrafish, the xanthophore, has been shown to depend upon the paired-box transcription factors Pax3 and Pax7a/b [59, 60]. Intriguingly, interactions between Pax3 and Mitf have been demonstrated in mammal melanocyte development [61]. At least some zebrafish xanthoblasts express *mitfa* [62] and we show that loss of *tfec* delays xanthoblast migration, raising the question of whether interplay between Mitfa and Tfec might be important for xanthoblast fate choice. Furthermore, it will be of interest to examine potential interactions between not only Tfec and Mitfa, but also between MiT and Pax transcription factors during chromatoblast diversification.

To conclude, our study contributes to deepening our understanding of the molecular basis of NC and pigment cell development in zebrafish, providing additional support for the progressive fate restriction of multipotent stem cells. While we show Tfec plays a key role in the GRNs underpinning NC maintenance and chromatophore specification, detailed assessment of the diversity of pigment progenitor states during embryonic stages is needed to test the hypothesis of a tripotent chromatoblast. Furthermore, focused effort on the (redundant) roles of transcription factors in xanthophore development will be decisive in understanding pigment cell fate choice in zebrafish.

Materials and methods

Ethics statement

This study was performed with the approval of the University of Bath ethics committee and in full accordance with the Animals (Scientific Procedures) Act 1986, under Home Office Project Licenses 30/2937 and P87C67227, and in compliance with protocol AM10125 approved by the Institutional Animal Care and Use Committee of Virginia Commonwealth University.

Zebrafish husbandry

All embryos were obtained from natural crosses. Staging was performed according to Kimmel et al (1995) [63]. WIK or NHGRI-1 wild-type embryos served as controls as indicated in each figure. The following mutant lines were examined: *sox10*^{l3} [20], *foxd3*^{zdf10} [29], *sox9b*^{fh313} [64,

65], *mitfa*^{w2} [21], *ltk*^{ty82} [11], *tfap2a*^{ts213} [66]. Adult fish were maintained in accordance to official guidelines: water temperature: 28°C, water pH: 7.4, conductivity: 800 mS, ammonia concentration: <0.1 mg/L, nitrite concentration: 0 mg/L, nitrate concentration: <5 mg/L, water hardness: 80–120 mg/L. The dark/light cycle was set at 10/14 hours. The adult stocking density was 5 fish/L, and the larvae stocking density <100 fish/L.

CRISPR mutagenesis

Target sequences for CRISPR/Cas9 mutagenesis were identified using version 1 of the CHOP-CHOP webtool (<http://chopchop.cbu.uib.no/>; [67]). The template for synthesis of the guide RNA (gRNA) was generated using a previously described PCR method [68]. Primer sequences are provided in Table 1.

The *tfec*^{ba6} and assorted *tfec*^{vc} alleles were generated independently as follows:

***tfec*^{ba6}.** 280 pg of CRISPR guide RNA mixed with 700 pg *Cas9* mRNA per embryo were injected at the flat cell stage. RNAs were diluted in RNase-free water. Approximately 200 injected embryos were raised, from which 30–40 pairs were in-crossed to screen for germ-line transmission. Adults that transmitted mutant alleles were separated and outcrossed wild-type fish of the WIK line to generate F1 offspring. F1 siblings (which conceivably could carry different mutant alleles) were in-crossed to identify mutation carriers. 3 fish were identified, which were outcrossed again to WIK fish and the resulting F2 generation raised. For all experiments the F2 of one of the three identified F1 fish were used. Screening was based on iridophore phenotype and confirmed by a High Resolution Melt Analysis (HRMA) assay for molecular screening (see below). To characterise the mutations, F1 adult genomic DNA extracted by swabbing and genomic DNA extracted from F2 embryos were sent for sequencing.

***tfec*^{vc} alleles.** CRISPR guide RNA was synthesized using the MEGAscript T7 Transcription Kit (Invitrogen; Cat# AM1354) and purified using the miRvana miRNA Isolation Kit (Invitrogen; Cat# AM1560) as described by [69]. Capped *Cas9* mRNA was generated from the plasmid pT3TS-nCas9n [69], a gift from Wenbiao Chen (Addgene plasmid; Cat# 46757) using the mMACHINE T3 Transcription Kit (Invitrogen; Cat# AM1348). *Cas9* mRNA and *tfec* exon 7 sgRNA were each diluted to 100 ng/μl for microinjection into one-cell embryos of the NHGRI-1 strain [70]. A fraction of the injected set was sacrificed for genomic DNA preparation [71] to evaluate the efficacy of the guide RNA using the primers *cex7F* and *cex7R*, followed by restriction digest with *StuI*, which cuts in the target sequence. The remaining injected embryos were raised to adulthood and intercrossed or mated to wild-type (NHGRI-1) partners. F1 carriers were identified using the PCR digest assay above, and undigested PCR products (representing mutant alleles) were purified and sequenced.

High resolution melt analysis. High Resolution Melting (HRM) Software V3.0.1 (Thermo Fisher Scientific) was used to detect and amplify differences between the melting temperature of 150–200 bp q-RT PCR amplicons generated from reference wild-type (WT) samples versus mutagenized embryos or adults. To perform q-RT PCR for HRMA, template genomic DNA was extracted using the KAPA Express Extract Kit (Sigma-Aldrich; Cat# KK7103) according to manufacturer's instructions, and was diluted to 8 ng/μl. Amplification reactions were set up as per manufacturer's instructions using KAPA HRM FAST reagents (Sigma-Aldrich; Cat# KK4201) and primers designed according to the relevant recommendations (Table 1). Following amplification, a continuous melt curve was generated by increasing the temperature from 60°C (1 min) to 95°C (15 sec) in 0.3°C/sec increments. To detect CRISPR/Cas9-mediated mutagenesis, at least 8 WT reference samples were included in the analysis.

Table 1. Oligonucleotides used in this study.

Name	Sequence (5' to 3')
tfecex7gR1T7	GCGTAATACGACTCACTATAGGCGATCCTCAAGGCCTCGGGTTTTAGAGCTAGAAATAGC
cex7F	AGGCAAGGTAATGTCCGAGA
cex7R	TGGATCCGTAGCTGGAGTCT
Hrma F	CTGGAACAAAGGGACGATCC
Hrma R	TGGATCCGTAGCTGGAGTCT

<https://doi.org/10.1371/journal.pone.0244794.t001>

Chromatophore counts

Melanocyte counts were performed at 30 hpf and at 4 dpf on anaesthetized or fixed embryos under transmitted light. Embryos at 4 dpf were treated with 2 μ M melatonin directly prior to counting. To count iridophores, PTU-treated embryos were observed under incident light. Pigment cell counts were made under a Zeiss Axio Zoom.V16 fluorescence stereo zoom microscope. Statistics on cell counts were performed on Microsoft Excel using unpaired two-tailed t-tests. Means were considered statistically different if the calculated p-value was less than 0.05

Cloning and rescue by plasmid microinjection

The full-length coding sequence of *tfec* was subcloned in-frame into the Gateway 3' Entry vector p3E-2A-FLAG-pA to make p3E-2A-FLAG-*tfec*-pA. A multisite Gateway LR+ cloning reaction was then carried out with this plasmid along with Tol2 Kit destination vector pDestTol2pA2 and entry vector pME-mCherry-no stop [72] and entry vector p5E-*tfec*2.4 [42]. Following bacterial transformation, correct clones were identified by restriction digest of mini-prep cultures.

The resulting plasmid (designated pDestTol2pA2-*tfec*2.4/mCherry-nostop/2A-FLAG-*tfec*-pA) at 25 ng/ μ l was co-injected with Tol2 transposase mRNA at 25 ng/ μ l into embryos from an intercross of heterozygous *tfec*^{vc60} carriers. Homozygous mutant embryos were identified between 48 and 72 hpf and scored at 96 hpf on a stereo dissection microscope under incident light for the presence of iridophores.

For overexpression experiments, the following additional plasmids were generated using multisite Gateway cloning and the entry vectors pENTR5'_ubi [73], p5E-sox10 [17], pME-EGFP [72] and pENTRDSRedEx2 [74]: pDestTol2pA2-ubi/mCherry-nostop/2A-FLAG-*tfec*-pA, pDestTol2pA2-ubi/EGFP/pA, pDestTol2pA2-sox10/mCherry-nostop/2A-FLAG-*mitfa*-pA, and pDestTol2pA2-sox10/DsRed/pA. These plasmids were injected as above at 25 ng/ μ l with 25 ng/ μ l Tol2 transposase mRNA. Iridophores were counted in the dorsal and ventral stripes of between 26 and 56 larvae.

Transcript detection in whole-mount embryos

Detailed information on the preparation of generic materials and the protocols for performing chromogenic whole-mount *in situ* hybridisation as well as multiplex fluorescent RNAscope can be found in Petratos et al. (2017) [75]. For whole-mount *in situ* hybridisation, the probes used were *sox10* [20], *foxd3* [76], *ltk* [11], *pnp4a* [17], *aox5* [62], *gch2* [62], *pou3f1/oct6* [77], *dlx2a* [78], *mitfa* [21] and *tfec* (NM_001030105.2; [14]). For multiplex RNAscope, the following probes were used: *ltk* (ACD; Cat# 444641), *tfec* (ACD; Cat# 444701).

Embryos were observed and imaged, and the Pearson's chi-squared test was used, as previously described [14], to process and statistically analyse results, to test the hypothesis that altered phenotypes correlated with homozygous mutations. *tfap2a* and *foxd3* mutant embryos

were identified using previously described genotyping protocols [29, 79] following imaging and preparation of genomic DNA [71].

Alcian blue staining and immunohistochemistry

Larvae from an intercross of *tfec*^{vc60} heterozygous adults were sorted at 4 days post-fertilization based on the iridophore phenotype, and then were fixed in separate tubes overnight in 4% PFA. Alcian blue staining was then carried out essentially as described [80]. Samples were imaged using an Olympus SZX12 stereomicroscope with DP70 camera.

Immunohistochemistry was carried out as previously described [77]. Primary monoclonal antibodies against HuC/D (Molecular Probes) and Pax7 (Developmental Studies Hybridoma Bank) were used at 1:500 and 1:20 respectively, and goat anti-mouse secondary antibodies conjugated to Alexa 568 or Alexa 488 (Molecular Probes) were each used at 1:750 dilution. For combined *tfec* whole-mount *in situ* hybridisation /Pax7 IHC, the Pax7 antibodies were added simultaneously with the anti-Fab fragments [81]. Samples were imaged on a Zeiss Axio Imager.M2 compound microscope with AxioCam 503 colour camera, processed using ZEN software and Adobe Photoshop CC 2018 and 2019.

Drug treatments

Larvae from an intercross of *tfec*^{vc60} heterozygous adults were treated with tyrphostin/AG1478 (LC Laboratories) at 2 μ M or DMSO from 8 hpf to 48 hpf, with or without the addition of MoTP (Enzo Life Sciences) at 50 μ M from 24 to 48 hpf, and examined at 4.5 dpf for recovery of melanocytes.

Supporting information

S1 Fig. Loss of *tfec* affects adult iridophore pigmentation. Compared to WT adult (A), G0 *tfec* crispant (mosaic) adult shows patches of iridophore loss on eye and flank (B). When two *tfec* CRISPR G0 founder fish were mated, almost all of the offspring lacking iridophores died as larvae, but one escaper survived to adulthood and the absence of iridophores persisted (C). Of the homozygous *tfec*^{vc60} embryos injected with a Tol2 transposon containing the *tfec* promoter and cDNA and Tol2 transposase mRNA, one survived to adulthood and displayed partial rescue of adult iridophore pigmentation (D). Scale bar: A-D: 0.5 cm; D: 0.35 cm. (TIF)

S2 Fig. Recovery of melanocyte development in *tfec* mutants is not dependent upon regeneration from adult melanocyte stem cells. (A,B) *tfec* homozygous mutant larvae treated with AG1478 (B) recover melanocytes to levels of DMSO-treated larvae (A) by 4.5 dpf. (C,D) Wild-type larvae, treated with MoTP reagent at an early stage to ablate melanocytes, and with AG1478 (D) show strongly reduced melanocyte numbers by 4.5 dpf, compared to MoTP and DMSO-treated siblings (C). Scale bar: 250 μ m. (TIF)

S3 Fig. The number of *tfec*⁺ and *pnp4a*⁺ cells is significantly reduced in *tfec* mutants. Positive cells were scored along the dorsal and the ventral stripe of known *tfec*^{ba6/ba6} embryos (red bars) and of wild-type or heterozygous siblings (green bars). *: p-value < 10⁻³. (TIF)

S4 Fig.
(TIF)

S1 Table. Additional information on the assessment of live embryonic phenotypes. For melanocyte counts at 4 dpf, to derive the average along the lateral stripe, the cells along both stripes of each embryo were independently scored. Presented p-values derived from unpaired two-tailed t-test between WT (or heterozygous for the melanocyte counts) and the genotype corresponding to each row. DS, dorsal stripe; DT, dorsal trunk; H, head; LS, lateral stripe; MP, migration paths; VS, ventral stripe; VT, ventral trunk.
(DOCX)

S2 Table. Statistics of loss of function experiments. The Pearson's chi-squared test for goodness of fit is used to calculate the likelihood of a non-WT phenotype, which is consistently present in a number of embryos (1st sub-column of each of the 4 developmental stages) within a batch of WT, heterozygous and homozygous mutant siblings, correlating with homozygosity of the mutant allele in those individuals. Due to the recessive nature of investigated alleles, 25% of embryos in each batch are expected to be homozygous mutants. Therefore, the p-value derived from the chi-squared test indicates whether the number of individuals with an alternative phenotype conform to the expected 25% (null hypothesis), with any deviation being attributable to random chance ($p > 0.1$), or whether the numbers deviate significantly from the expected ($p \leq 0.1$; null hypothesis is rejected). Where observed phenotypes did not significantly correlate with expected Mendelian ratios, i.e. where there is unlikely to be a mutant phenotype, the corresponding counts and p-values are red and bold. For the data on *sox10*^{t3/t3}; *sox9b*^{fh313/fh313} double mutants, the orange cells indicate how many embryos in the sample showed the known *sox9b*^{fh313/fh313} phenotype, the green cells indicate number of embryos with the *sox10*^{t3/t3} phenotype and blue cells indicate unexpected alternative phenotypes, likely owed to double loss of function.
(DOCX)

Author Contributions

Conceptualization: Robert N. Kelsh, James A. Lister.

Data curation: Kleio Petratou.

Formal analysis: James A. Lister.

Funding acquisition: Robert N. Kelsh, James A. Lister.

Investigation: Kleio Petratou, Samantha A. Spencer, James A. Lister.

Methodology: Kleio Petratou, Samantha A. Spencer, James A. Lister.

Supervision: Robert N. Kelsh, James A. Lister.

Writing – original draft: Kleio Petratou, Samantha A. Spencer, James A. Lister.

Writing – review & editing: Kleio Petratou, Robert N. Kelsh, James A. Lister.

References

1. Hoekstra H. E., "Genetics, development and evolution of adaptive pigmentation in vertebrates," *Heredity*, vol. 97, no. 3, pp. 222–234, 2006. <https://doi.org/10.1038/sj.hdy.6800861> PMID: 16823403
2. Parichy D. M. and Spiewak J. E., "Origins of adult pigmentation: diversity in pigment stem cell lineages and implications for pattern evolution.," *Pigment cell & melanoma research*, vol. 28, no. 1, pp. 31–50, 2015. <https://doi.org/10.1111/pcmr.12332> PMID: 25421288
3. Schartl M., Larue L., Goda M., Bosenberg M. W., Hashimoto H., and Kelsh R. N., "What is a vertebrate pigment cell?," *Pigment Cell & Melanoma Research*, vol. 29, no. 1, pp. 8–14, 2016. <https://doi.org/10.1111/pcmr.12409> PMID: 26247887

4. Sieber-Blum M. and Cohen A. M., "Clonal analysis of quail neural crest cells: They are pluripotent and differentiate in vitro in the absence of noncrest cells," *Developmental Biology*, vol. 80, no. 1, pp. 96–106, 1980. [https://doi.org/10.1016/0012-1606\(80\)90501-1](https://doi.org/10.1016/0012-1606(80)90501-1) PMID: 7439536
5. Weston J. A., "Sequential segregation and fate of developmentally restricted intermediate cell populations in the neural crest lineage," *Current topics in developmental biology*, vol. 25, pp. 133–53, 1991. [https://doi.org/10.1016/s0070-2153\(08\)60414-7](https://doi.org/10.1016/s0070-2153(08)60414-7) PMID: 1660392
6. Le Douarin N., Dulac C., Dupin E., and Cameron-Curry P., "Glial cell lineages in the neural crest," *Glia*, vol. 4, no. 2, pp. 175–184, 1991. <https://doi.org/10.1002/glia.440040209> PMID: 1827777
7. Serbedzija G. N., Bronner-Fraser M., and Fraser S. E., "Developmental potential of trunk neural crest cells in the mouse," *Development (Cambridge, England)*, vol. 120, no. 7, pp. 1709–18, 1994. PMID: 7523054
8. Calloni G. W., Le Douarin N. M., and Dupin E., "High frequency of cephalic neural crest cells shows coexistence of neurogenic, melanogenic, and osteogenic differentiation capacities," *Proceedings of the National Academy of Sciences of the United States of America*, vol. 106, no. 22, pp. 8947–8952, 2009. <https://doi.org/10.1073/pnas.0903780106> PMID: 19447928
9. Soldatov R., Kaucka M., Kastriiti M. E., Petersen J., Chontorotzea T., Englmaier L., et al., "Spatiotemporal structure of cell fate decisions in murine neural crest," *Science*, vol. 364, no. 6444, 2019. <https://doi.org/10.1126/science.aas9536> PMID: 31171666
10. Raible D. W. and Eisen J. S., "Restriction of neural crest cell fate in the trunk of the embryonic zebrafish," *Development*, vol. 120, pp. 495–503, 1994. PMID: 8162850
11. Lopes S. S., Yang X., Müller J., Carney T. J., McAdow A. R., Rauch G.-J., et al., "Leukocyte Tyrosine Kinase Functions in Pigment Cell Development," *PLoS Genetics*, vol. 4, no. 3, p. 13, 2008. <https://doi.org/10.1371/journal.pgen.1000026> PMID: 18369445
12. Singh A. P., Dinwiddie A., Mahalwar P., Schach U., Linker C., Irion U., et al., "Pigment Cell Progenitors in Zebrafish Remain Multipotent through Metamorphosis," *Developmental Cell*, vol. 38, no. 3, pp. 316–330, 2016. <https://doi.org/10.1016/j.devcel.2016.06.020> PMID: 27453500
13. Greenhill E. R., Rocco A., Vibert L., Nikaido M., and Kelsh R. N., "An Iterative Genetic and Dynamical Modelling Approach Identifies Novel Features of the Gene Regulatory Network Underlying Melanocyte Development," *PLoS Genetics*, vol. 7, no. 9, p. 18, 2011. <https://doi.org/10.1371/journal.pgen.1002265> PMID: 21909283
14. Petratou K., Subkhankulova T., Lister J. A., Rocco A., Schwetlick H., and Kelsh R. N., "A systems biology approach uncovers the core gene regulatory network governing iridophore fate choice from the neural crest," *PLoS Genetics*, vol. 14, no. 10, 2018. <https://doi.org/10.1371/journal.pgen.1007402> PMID: 30286071
15. Bagnara J. T., Matsumoto J., Ferris W., Frost S. K., Turner W. A., Tchen T. T., et al., "Common origin of pigment cells," *Science*, vol. 203, no. 4379, pp. 410–415, 1979. <https://doi.org/10.1126/science.760198> PMID: 760198
16. Curran K., Raible D. W., and Lister J. A., "Foxd3 controls melanophore specification in the zebrafish neural crest by regulation of Mitf," *Developmental Biology*, vol. 332, no. 2, pp. 408–417, 2009. <https://doi.org/10.1016/j.ydbio.2009.06.010> PMID: 19527705
17. Curran K., Lister J. A., Kunkel G. R., Prendergast A., Parichy D. M., and Raible D. W., "Interplay between Foxd3 and Mitf regulates cell fate plasticity in the zebrafish neural crest," *Developmental Biology*, vol. 344, no. 1, pp. 107–118, 2010. <https://doi.org/10.1016/j.ydbio.2010.04.023> PMID: 20460180
18. Kelsh R. N., Brand M., Jiang Y. J., Heisenberg C. P., Lin S., Haffter P., et al., "Zebrafish pigmentation mutations and the processes of neural crest development," *Development*, vol. 123, no. 1, pp. 369–389, 1996. PMID: 9007256
19. Kelsh R. N. and Eisen J. S., "The zebrafish colourless gene regulates development of non-ectomesenchymal neural crest derivatives," *Development*, vol. 127, no. 3, pp. 2581–2590, 2000. PMID: 10631172
20. Dutton K. A., Pauliny A., Lopes S. S., Elworthy S., Carney T. J., Rauch J., et al., "Zebrafish colourless encodes sox10 and specifies non-ectomesenchymal neural crest fates," *Development*, vol. 128, no. 21, pp. 4113–4125, 2001. PMID: 11684650
21. Lister J. A., Robertson C. P., Lepage T., Johnson S. L., and Raible D. W., "nacre encodes a zebrafish microphthalmia-related protein that regulates neural-crest-derived pigment cell fate," *Development*, vol. 126, no. 17, pp. 3757–3767, 1999. PMID: 10433906
22. Carney T. J., Dutton K. A., Greenhill E., Delfino-Machín M., Dufourcq P., Blader P., et al., "A direct role for Sox10 in specification of neural crest-derived sensory neurons," *Development (Cambridge, England)*, vol. 133, no. 23, pp. 4619–30, 2006. <https://doi.org/10.1242/dev.02668> PMID: 17065232
23. Delfino-Machín M., Madelaine R., Busolin G., Nikaido M., Colanesi S., Camargo-Sosa K., et al., "Sox10 contributes to the balance of fate choice in dorsal root ganglion progenitors," *PLOS ONE*, vol. 12, no. 3, p. e0172947, 2017. <https://doi.org/10.1371/journal.pone.0172947> PMID: 28253350

24. Dorsky R. I., Raible D. W., and Moon R. T., "Direct regulation of nacre, a zebrafish MITF homolog required for pigment cell formation, by the Wnt pathway," *Genes & Development*, vol. 14, no. 2, pp. 158–162, 2000. PMID: [10652270](#)
25. Elworthy S., Lister J. A., Carney T. J., Raible D. W., and Kelsh R. N., "Transcriptional regulation of mitfa accounts for the sox10 requirement in zebrafish melanophore development.," *Development*, vol. 130, no. 12, pp. 2809–2818, 2003. <https://doi.org/10.1242/dev.00461> PMID: [12736222](#)
26. Vibert L., Aquino G., Gehring I., Subkankulova T., Schilling T. F., Rocco A., et al., "An ongoing role for Wnt signaling in differentiating melanocytes in vivo," *Pigment Cell & Melanoma Research*, vol. 30, no. 2, pp. 219–232, 2017. <https://doi.org/10.1111/pcmr.12568> PMID: [27977907](#)
27. Seberg H. E., Van Otterloo E., Loftus S. K., Liu H., Bonde G., Sompallae R., et al., "TFAP2 paralogs regulate melanocyte differentiation in parallel with MITF," *PLOS Genetics*, vol. 13, no. 3, p. e1006636, 2017. <https://doi.org/10.1371/journal.pgen.1006636> PMID: [28249010](#)
28. Montero-Balaguer M., Lang M. R., Sachdev S. W., Knappmeyer C., Stewart R. A., De La Guardia A., et al., "The mother superior mutation ablates foxd3 activity in neural crest progenitor cells and depletes neural crest derivatives in zebrafish.," *Developmental dynamics an official publication of the American Association of Anatomists*, vol. 235, no. 12, pp. 3199–3212, 2006. <https://doi.org/10.1002/dvdy.20959> PMID: [17013879](#)
29. Stewart R. A., Arduini B. L., Berghmans S., George R. E., Kanki J. P., Henion P. D., et al., "Zebrafish foxd3 is selectively required for neural crest specification, migration and survival.," *Developmental Biology*, vol. 292, no. 1, pp. 174–188, 2006. <https://doi.org/10.1016/j.ydbio.2005.12.035> PMID: [16499899](#)
30. Cooper C. D., Linbo T. H., and Raible D. W., "Kit and foxd3 genetically interact to regulate melanophore survival in zebrafish.," *Developmental Dynamics*, vol. 238, no. 4, pp. 875–886, 2009. <https://doi.org/10.1002/dvdy.21910> PMID: [19301400](#)
31. Lukoseviciute M., Gavriouchkina D., Williams R. M., Hochgreb-Hagele T., Senanayake U., Chong-Morrison V., et al., "From Pioneer to Repressor: Bimodal foxd3 Activity Dynamically Remodels Neural Crest Regulatory Landscape In Vivo," *Developmental Cell*, vol. 47, no. 5, p. 608–628.e6, 2018. <https://doi.org/10.1016/j.devcel.2018.11.009> PMID: [30513303](#)
32. Ng A., Uribe R. A., Yieh L., Nuckels R., and Gross J. M., "Zebrafish mutations in gart and paics identify crucial roles for de novo purine synthesis in vertebrate pigmentation and ocular development.," *Development (Cambridge, England)*, vol. 136, no. 15, pp. 2601–11, 2009.
33. Clancey L. F., Beirl A. J., Linbo T. H., and Cooper C. D., "Maintenance of Melanophore Morphology and Survival Is Cathepsin and vps11 Dependent in Zebrafish," *PLoS ONE*, vol. 8, no. 5, 2013. <https://doi.org/10.1371/journal.pone.0065096> PMID: [23724125](#)
34. Krauss J., Astrinidis P., Astrinides P., Frohnhöfer H. G., Walderich B., and Nüsslein-Volhard C., "Transparent, a gene affecting stripe formation in Zebrafish, encodes the mitochondrial protein Mpv17 that is required for iridophore survival.," *Biology open*, vol. 2, no. 7, pp. 703–10, 2013. <https://doi.org/10.1242/bio.20135132> PMID: [23862018](#)
35. D'Agati G., Beltre R., Sessa A., Burger A., Zhou Y., Mosimann C., et al., "A defect in the mitochondrial protein Mpv17 underlies the transparent casper zebrafish," *Developmental Biology*, vol. 430, no. 1, pp. 11–17, 2017. <https://doi.org/10.1016/j.ydbio.2017.07.017> PMID: [28760346](#)
36. Rodrigues F. S. L. M., Yang X., Nikaido M., Liu Q., and Kelsh R. N., "A Simple, Highly Visual in Vivo Screen for Anaplastic Lymphoma Kinase Inhibitors," *ACS Chemical Biology*, vol. 7, no. 12, pp. 1968–1974, 2012. <https://doi.org/10.1021/cb300361a> PMID: [22985331](#)
37. Fadeev A., Krauss J., Singh A. P., and Nüsslein-Volhard C., "Zebrafish Leucocyte tyrosine kinase controls iridophore establishment, proliferation and survival.," *Pigment cell & melanoma research*, vol. 29, no. 3, pp. 284–96, 2016. <https://doi.org/10.1111/pcmr.12454> PMID: [26801003](#)
38. Mo E. S., Cheng Q., Reshetnyak A. V., Schlessinger J., and Nicoli S., "Alk and Ltk ligands are essential for iridophore development in zebrafish mediated by the receptor tyrosine kinase Ltk," *Proceedings of the National Academy of Sciences of the United States of America*, vol. 114, no. 45, pp. 12027–12032, 2017. <https://doi.org/10.1073/pnas.1710254114> PMID: [29078341](#)
39. Lister J. A., Lane B. M., Nguyen A., and Lunney K., "Embryonic expression of zebrafish MIT family genes tfe3b, tfeb, and tfec.," *Developmental Dynamics*, vol. 240, no. 11, pp. 2529–38, 2011. <https://doi.org/10.1002/dvdy.22743> PMID: [21932325](#)
40. Higdon C. W., Mitra R. D., and Johnson S. L., "Gene expression analysis of zebrafish melanocytes, iridophores, and retinal pigmented epithelium reveals indicators of biological function and developmental origin.," *PLoS One*, vol. 8, no. 7, p. e67801, 2013. <https://doi.org/10.1371/journal.pone.0067801> PMID: [23874447](#)
41. Simões-Costa M., Bronner M. E., Agarwal P., Verzi M. P., Nguyen T., Hu J., et al., "Establishing neural crest identity: a gene regulatory recipe.," *Development (Cambridge, England)*, vol. 142, no. 2, pp. 242–57, 2015. <https://doi.org/10.1242/dev.105445> PMID: [25564621](#)

42. Miesfeld J. B., Gestri G., Clark B. S., Flinn M. A., Poole R. J., Bader J. R., et al., "Yap and Taz regulate retinal pigment epithelial cell fate," *Development (Cambridge)*, vol. 142, no. 17, pp. 3021–3032, 2015. <https://doi.org/10.1242/dev.119008> PMID: 26209646
43. Budi E. H., Patterson L. B., and Parichy D. M., "Embryonic requirements for ErbB signaling in neural crest development and adult pigment pattern formation.," *Development*, vol. 135, no. 15, pp. 2603–2614, 2008. <https://doi.org/10.1242/dev.019299> PMID: 18508863
44. Hultman K. A., Budi E. H., Teasley D. C., Gottlieb A. Y., Parichy D. M., and Johnson S. L., "Defects in ErbB-Dependent Establishment of Adult Melanocyte Stem Cells Reveal Independent Origins for Embryonic and Regeneration Melanocytes," *PLoS Genetics*, vol. 5, no. 7, p. 13, 2009. <https://doi.org/10.1371/journal.pgen.1000544> PMID: 19578401
45. Saunders L. M., Mishra A. K., Aman A. J., Lewis V. M., Toomey M. B., Packer J. S., et al., "Thyroid hormone regulates distinct paths to maturation in pigment cell lineages," *eLife*, vol. 8, e45181, 2019. <https://doi.org/10.7554/eLife.45181> PMID: 31140974
46. Mahony C. B., Fish R. J., Pasche C., and Bertrand J. Y., "tfec controls the hematopoietic stem cell vascular niche during zebrafish embryogenesis.," *Blood*, vol. 128, no. 10, pp. 1336–45, 2016. <https://doi.org/10.1182/blood-2016-04-710137> PMID: 27402973
47. Bharti K., Gasper M., Ou J., Brucato M., Clore-Gronenborn K., Pickel J., et al., "A regulatory loop involving PAX6, MITF, and WNT signaling controls retinal pigment epithelium development," *PLoS Genetics*, vol. 8, no. 7, 2012.
48. Sinagoga K. L., Larimer-Picciani A. M., George S. M., Spencer S. A., Lister J. A., and Gross J. M., "Mitf-family transcription factor function is required within cranial neural crest cells to promote choroid fissure closure," *Development*, p. dev. 187047, 2020. <https://doi.org/10.1242/dev.187047> PMID: 32541011
49. Arduini B. L., Bosse K. M., and Henion P. D., "Genetic ablation of neural crest cell diversification.," *Development (Cambridge, England)*, vol. 136, no. 12, pp. 1987–94, 2009. <https://doi.org/10.1242/dev.033209> PMID: 19439494
50. Cheung M. and Briscoe J., "Neural crest development is regulated by the transcription factor Sox9.," *Development (Cambridge, England)*, vol. 130, no. 23, pp. 5681–93, 2003. <https://doi.org/10.1242/dev.00808> PMID: 14522876
51. Betancur P., Bronner-Fraser M., and Sauka-Spengler T., "Genomic code for Sox10 activation reveals a key regulatory enhancer for cranial neural crest.," *Proceedings of the National Academy of Sciences of the United States of America*, vol. 107, no. 8, pp. 3570–5, 2010. <https://doi.org/10.1073/pnas.0906596107> PMID: 20139305
52. Li W. and Cornell R. A., "Redundant activities of Tfp2a and Tfp2c are required for neural crest induction and development of other non-neural ectoderm derivatives in zebrafish embryos," *Developmental Biology*, vol. 304, no. 1, pp. 338–354, 2007. <https://doi.org/10.1016/j.ydbio.2006.12.042> PMID: 17258188
53. Wang W. Der, Melville D. B., Montero-Balaguer M., Hatzopoulos A. K., and Knapik E. W., "Tfp2a and Foxd3 regulate early steps in the development of the neural crest progenitor population," *Developmental Biology*, vol. 360, no. 1, pp. 173–185, 2011. <https://doi.org/10.1016/j.ydbio.2011.09.019> PMID: 21963426
54. Dooley C. M., Wali N., Sealy I. M., White R. J., Stemple D. L., Collins J. E., et al., "The gene regulatory basis of genetic compensation during neural crest induction," *PLOS Genetics*, vol. 15, no. 6, p. e1008213, 2019. <https://doi.org/10.1371/journal.pgen.1008213> PMID: 31199790
55. Knight R. D., Javidan Y., Nelson S., Zhang T., and Schilling T., "Skeletal and pigment cell defects in the lockjaw mutant reveal multiple roles for zebrafish tfp2a in neural crest development.," *Developmental Dynamics*, vol. 229, no. 1, pp. 87–98, 2004. <https://doi.org/10.1002/dvdy.10494> PMID: 14699580
56. Ignatius M. S., Moose H. E., El-Hodiri H. M., and Henion P. D., "colgate/hdac1 Repression of foxd3 expression is required to permit mitfa-dependent melanogenesis.," *Developmental Biology*, vol. 313, no. 2, pp. 568–583, 2008. <https://doi.org/10.1016/j.ydbio.2007.10.045> PMID: 18068699
57. Hemesath T. J., Steingrímsson E., McGill G., Hansen M. J., Vaught J., Hodgkinson C. A., et al., "microphthalmia, a critical factor in melanocyte development, defines a discrete transcription factor family.," *Genes & development*, vol. 8, no. 22, pp. 2770–80, 1994. <https://doi.org/10.1101/gad.8.22.2770> PMID: 7958932
58. Pogenberg V., Ögmundsdóttir M. H., Bergsteinsdóttir K., Schepsky A., Phung B., Deineko V., et al., "Restricted leucine zipper dimerization and specificity of DNA recognition of the melanocyte master regulator MITF," *Genes and Development*, vol. 26, no. 23, pp. 2647–2658, 2012. <https://doi.org/10.1101/gad.198192.112> PMID: 23207919
59. Minchin J. E. N. and Hughes S. M., "Sequential actions of Pax3 and Pax7 drive xanthophore development in zebrafish neural crest.," *Developmental Biology*, vol. 317, no. 2, pp. 508–522, 2008. <https://doi.org/10.1016/j.ydbio.2008.02.058> PMID: 18417109

60. Nord H., Dennhag N., Muck J., and Von Hofsten J., "Pax7 is required for establishment of the xanthophore lineage in zebrafish embryos," *Molecular Biology of the Cell*, vol. 27, no. 11, pp. 1853–1862, 2016. <https://doi.org/10.1091/mbc.E15-12-0821> PMID: 27053658
61. Lang D., Lu M. M., Huang L., Engleka K. A., Zhang M., Chu E. Y., et al., "Pax3 functions at a nodal point in melanocyte stem cell differentiation," *Nature*, vol. 433, no. 7028, pp. 884–887, 2005. <https://doi.org/10.1038/nature03292> PMID: 15729346
62. Parichy D. M., Ransom D. G., Paw B., Zon L. I., and Johnson S. L., "An orthologue of the kit-related gene *fms* is required for development of neural crest-derived xanthophores and a subpopulation of adult melanocytes in the zebrafish, *Danio rerio*," *Development*, vol. 127, no. 14, pp. 3031–3044, 2000. PMID: 10862741
63. Kimmel C. B., Ballard W. W., Kimmel S. R., Ullmann B., and Schilling T. F., "Stages of embryonic development of the zebrafish," *Developmental dynamics*, vol. 203, no. 3, pp. 253–310, 1995. <https://doi.org/10.1002/aja.1002030302> PMID: 8589427
64. Manfroid I., Ghaye A., Naye F., Detry N., Palm S., Pan L., et al., "Zebrafish *sox9b* is crucial for hepatopancreatic duct development and pancreatic endocrine cell regeneration," *Developmental Biology*, vol. 366, no. 2, pp. 268–78, 2012. <https://doi.org/10.1016/j.ydbio.2012.04.002> PMID: 22537488
65. Delous M., Yin C., Shin D., Ninov N., Debrito Carten J., Pan L., et al., "*sox9b* is a key regulator of pancreaticobiliary ductal system development," *PLoS Genetics*, vol. 8, no. 6, 2012. <https://doi.org/10.1371/journal.pgen.1002754> PMID: 22719264
66. Schilling T. F., Piotrowski T., Grandel H., Brand M., Heisenberg C. P., Jiang Y. J., et al., "Jaw and branchial arch mutants in zebrafish I: Branchial arches," *Development*, vol. 123, pp. 329–344, 1996. PMID: 9007253
67. Montague T. G., Cruz J. M., Gagnon J. A., Church G. M., and Valen E., "CHOPCHOP: A CRISPR/Cas9 and TALEN web tool for genome editing," *Nucleic Acids Research*, vol. 42, no. W1, 2014. <https://doi.org/10.1093/nar/gku410> PMID: 24861617
68. Talbot J. C. and Amacher S. L., "Supplementary methods: A streamlined CRISPR pipeline to reliably generate zebrafish frameshifting alleles," *Zebrafish*, vol. 11, no. 6, 2014.
69. Jao L. E., Wente S. R., and Chen W., "Efficient multiplex biallelic zebrafish genome editing using a CRISPR nuclease system," *Proceedings of the National Academy of Sciences of the United States of America*, vol. 110, no. 34, pp. 13904–13909, 2013. <https://doi.org/10.1073/pnas.1308335110> PMID: 23918387
70. Lafave M. C., Varshney G. K., Vemulapalli M., Mullikin J. C., and Burgess S. M., "A Defined Zebrafish Line for High-Throughput Genetics and Genomics: NHGRI-1," *Genetics Society of America*, pp. 167–170, 11-Apr-2014. <https://doi.org/10.1534/genetics.114.166769> PMID: 25009150
71. Meeker N. D., Hutchinson S. A., Ho L., and Trede N. S., "Method for isolation of PCR-ready genomic DNA from zebrafish tissues," *BioTechniques*, vol. 43, no. 5, pp. 610–614, 2007. <https://doi.org/10.2144/000112619> PMID: 18072590
72. Kwan K. M., Fujimoto E., Grabher C., Mangum B. D., Hardy M. E., Campbell D. S., et al., "The Tol2kit: A multisite gateway-based construction Kit for Tol2 transposon transgenesis constructs," *Developmental Dynamics*, vol. 236, no. 11, pp. 3088–3099, 2007. <https://doi.org/10.1002/dvdy.21343> PMID: 17937395
73. Mosimann C., Kaufman C. K., Li P., Pugach E. K., Tamplin O. J., and Zon L. I., "Ubiquitous transgene expression and Cre-based recombination driven by the ubiquitin promoter in zebrafish," *Development*, vol. 138, no. 1, pp. 169–177, 2011. <https://doi.org/10.1242/dev.059345> PMID: 21138979
74. Villefranc J. A., Amigo J., and Lawson N. D., "Gateway compatible vectors for analysis of gene function in the zebrafish," *Developmental Dynamics*, vol. 236, no. 11, pp. 3077–3087, 2007. <https://doi.org/10.1002/dvdy.21354> PMID: 17948311
75. Petratou K., Sosa K. C., Al Jabri R., Nagao Y., and Kelsh R. N., "Neural Crest Methodologies in Zebrafish and Medaka: Transcript and protein detection methodologies for neural crest research on whole mount zebrafish and medaka." Springer, 20-Dec-2017. <https://doi.org/10.1111/pcmr.12580> PMID: 28182333
76. Odenthal J. and Nüsslein-Volhard C., "fork head domain genes in zebrafish," *Development Genes and Evolution*, vol. 208, no. 5, pp. 245–58, 1998. <https://doi.org/10.1007/s004270050179> PMID: 9683740
77. Lister J. A., Cooper C., Nguyen K., Modrell M., Grant K., and Raible D. W., "Zebrafish *Foxd3* is required for development of a subset of neural crest derivatives," *Developmental Biology*, vol. 159, no. 1, pp. 50–59, 2006. <https://doi.org/10.1016/j.ydbio.2005.11.014> PMID: 16364284
78. Akimenko M. A., Ekker M., Wegner J., Lin W., and Westerfield M., "Combinatorial expression of three zebrafish genes related to distal-less: Part of a homeobox gene code for the head," *Journal of*

Neuroscience, vol. 14, no. 6, pp. 3475–3486, 1994. <https://doi.org/10.1523/JNEUROSCI.14-06-03475.1994> PMID: 7911517

79. Knight R. D., Nair S., Nelson S. S., Afshar A., Javidan Y., Geisler R., et al., “lockjaw encodes a zebrafish tfap2a required for early neural crest development.” *Development*, vol. 130, no. 23, pp. 5755–5768, 2003. <https://doi.org/10.1242/dev.00575> PMID: 14534133
80. Walker M. B. and Kimmel C. B., “A two-color acid-free cartilage and bone stain for zebrafish larvae,” *Biotechnic and Histochemistry*, vol. 82, no. 1, pp. 23–28, 2007. <https://doi.org/10.1080/10520290701333558> PMID: 17510811
81. Van Otterloo E., Li W., Bonde G., Day K. M., Hsu M.-Y., and Cornell R. A., “Differentiation of zebrafish melanophores depends on transcription factors AP2 alpha and AP2 epsilon.” *PLoS genetics*, vol. 6, no. 9, p. e1001122, 2010. <https://doi.org/10.1371/journal.pgen.1001122> PMID: 20862309